

**EARTH OBSERVATION of
OCEAN ACIDIFICATION:**

The case of Nusa Penida, Kelungkung, East Bali

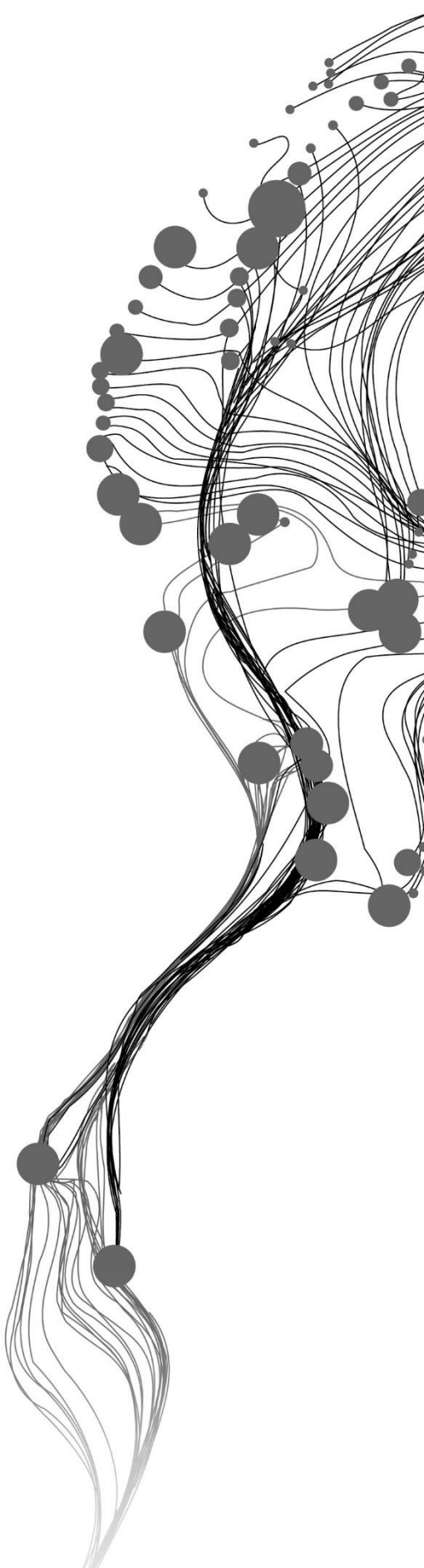
FAJAR EKO PRIYANTO

February, 2019

SUPERVISORS:

Dr. ir. S. Salama

Dr. ir. C. M. M. Mannaerts



EARTH OBSERVATION of OCEAN ACIDIFICATION:

The case of Nusa Penida, Kelungkung, East Bali

Submitted by:

FAJAR EKO PRIYANTO

S6036074

Enschede, The Netherlands, February 2019

SUPERVISORS:

Dr. ir. S. Salama

Dr. ir. C. M. M. Mannaerts

REPORT ASSESSMENT BOARD:

Dr. ir. C. Van der Tol (Chairman)

Dr. A. Hommersom (External Examiner, WaterInsight)

Submitted to:

Department of Water Resources and Environmental
Management (WREM)

Faculty of Geo-Information Science and Earth Observation,
University of Twente, The Netherlands

DISCLAIMER

This document describes work undertaken as part of a programme of study at the Faculty of Geo-Information Science and Earth Observation of the University of Twente. All views and opinions expressed therein remain the sole responsibility of the author, and do not necessarily represent those of the Faculty.

ABSTRACT

In this century, increasing carbon dioxide anthropogenic concentration in the atmosphere becomes an important issue which causes environmental problems such as global warming and ocean acidification. Oceans are known to act as a buffer in the ocean acidification. The key marine organisms such as fish and coral reef could diminish due to the difficulty to survive and sustain because of ocean acidification. Bali, an island in Indonesia has a good quality of coral cover can also be affected by ocean acidification.

Monitoring the Sea Surface Total Alkalinity would help us to know how far our ocean can survive from additional acid due to ocean acidification. It could give us a better understanding of the correlation between ocean acidification and ecological condition. This study will help the stakeholders for mapping the vulnerable areas and determine the necessary mitigation criteria regarding ocean acidification.

The aim of this study is to quantify the ocean acidification in Indonesian ocean, particularly in Nusa Penida, Bali using earth observation data for 1 year. The study generates a local model based on global Sea Surface Total Alkalinity Model where the sea surface salinity (SSS) as input parameters were retrieved from CMEMs product (SMOS satellite) and the sea surface temperature (SST) were obtained from the Sentinel-3 satellite. The result shows that the local model of Sea Surface Total Alkalinity is able to estimate the total alkalinity concentration on the dry season with 0.8 R^2 . The reliability of this local model of Sea Surface Total Alkalinity was assessed with a chemical model using Aqion/Phreeqc software.

Keywords:

Ocean Acidification, Total Alkalinity, Sea Surface Salinity (SSS), Sea Surface Temperature (SST), and Sea Surface Total Alkalinity Model.

ACKNOWLEDGMENTS

With the completion of this master's thesis, I would like to express my gratitude to everyone who have supported me through my master study.

Special acknowledgement to the Ministry of Research Technology, and Higher Education of Indonesia from which I received the Riset-Pro scholarship. Through this scholarship I had financial support to pursue my master study in ITC, University of Twente. I also thank the Agency of the Assessment and Application of Technology (BPPT) for their permit given to me to do my study.

I would like to express my sincere gratitude to my thesis supervisor Dr. ir. S. Salama and Dr. ir. C. M. M. Mannaerts for the new insights, support, advice, and feedbacks in every part of my research and thesis writing.

I would like to thanks to the Copernicus for giving me an access to the satellite data. And also Balai Riset dan Observasi Laut (BROL) from the Ministry of Maritime Affairs and Fisheries of Indonesia for providing me the instrument and nutrient data.

Thanks for the technical support from Rizki Hanintyo, Ratna Mayasari, and Aji Putra Perdana whenever I encountered problems with the software. Thanks to also for Aulia Akbar, Kamia Handayani, and Kunaifi for suggestion in improving my writing on the thesis report. I also owe incredible thanks to all Indonesian fellow students in Enschede for support and help during my master programme. Also, for all my classmate from WREM department, thank you for sharing the wonderful working and studying experience.

Finally and foremost, I would like to thank my beloved family, my lovely wife Miranti Budi Kusumawati, my daughter Affaf Atira Fara Putri, and my son Bilal Ramadhan Rafa Putra for endless love, support and encouragement. Also, thanks to my parents, Bapak Sudarminto and Yatemi, who always inspires and supports me emotionally.

TABLE OF CONTENTS

Abstract.....	i
Acknowledgments.....	ii
List of figures.....	iv
List of tables.....	v
Acronyms.....	vi
1. Introduction.....	1
1.1. Background.....	1
1.2. Research Problem.....	4
1.3. Justification.....	5
1.4. Research Objectives and Questions.....	5
1.4.1. General Objective.....	5
1.4.2. Specific Objective.....	5
1.4.3. Research Questions.....	5
1.5. Study Area.....	6
2. Methodology.....	7
2.1. Work Flow.....	7
2.2. Fieldwork.....	8
2.2.1. General Description.....	8
2.2.2. Measurement Procedure.....	9
2.2.3. In-Situ Measurement.....	10
2.3. Remote Sensing Data.....	15
2.3.1. General Description.....	15
2.3.2. Reprocessing Satellite Data.....	15
3. Analysis.....	18
3.1. Fieldwork Data Analysis.....	18
3.2. Satellite Data Analysis.....	19
3.3. Aquatic Chemistry Validation Using Aqion/Phreeqc.....	20
3.4. Total Alkalinity Model Calibration and Validation.....	21
4. Result and Discussion.....	25
4.1. Result.....	25
4.1.1. Remote Sensing Modelling Result.....	25
4.1.2. Hydrogeochemical Modelling Result.....	30
4.2. Discussion.....	33
4.2.1. La-Nina El-Nino.....	33
4.2.2. Monsoon.....	34
4.2.3. Madden-Julian Oscillation.....	35
4.2.4. Indonesian Through Flow.....	36
4.2.5. Sea Surface Total Alkalinity Variability.....	37
4.2.6. Future Prediction of Total Alkalinity.....	38
5. Conclusion and Recommendation.....	40
5.1. Conclusion.....	40
5.2. Recommendation.....	41
List of references.....	43
APPENDICES.....	46

LIST OF FIGURES

Figure 1. Ocean acidification process on the seawater (Ritter, 2016).....	1
Figure 2. Global aragonite saturation distribution in August 2005.(Takahashi et al., 2014)	2
Figure 3. Average pH in the Indonesian ocean using Hamburg Shelf Ocean Model (HAMSOM) for 1992-2009 (Putri, 2015).....	4
Figure 4. Experimental model for Total alkalinity concentration ($\mu\text{mol}/\text{kg}$) in Greater Caribbean Region on 2012(NOAA, 2014).	4
Figure 5. In-situ measurement trajectory.....	6
Figure 6. The flow chart of the methodology for the study.....	7
Figure 7. Sampling point on this research.....	8
Figure 8. Instrument preparation (left) and WQC-TOA DKK measurement (right).	9
Figure 9. Seawater sampling (left) and Total Alkalinity measurement (right).	9
Figure 10. Instrument used for field measurement in this research are TOA-DKK WQC 24 (left), Garmin GPSMAP sounder (middle) and Trios Ramses (Right).	10
Figure 11. pH field measurement distribution.	11
Figure 12. Total alkalinity field measurement distribution.	11
Figure 13. Salinity consistency measurement between WQC and refractometer.	12
Figure 14. Salinity field measurement distribution.....	13
Figure 15. Field measurement of temperature distribution.....	13
Figure 16. Sentinel 3 ARC SST data product at 14 October 2018.....	15
Figure 17. SMOS salinity (level 2) data on 15 October 2018.....	16
Figure 18. CMEMs salinity (SMOS level 4) product.....	17
Figure 19. Histogram analysis on each parameter.....	19
Figure 20. Local model calibration result.....	22
Figure 21. Local model validation result.	23
Figure 22. Local model assessment.	24
Figure 23. Total alkalinity results from satellite data on 15 October 2018.	25
Figure 24. Local model satellite validation.	26
Figure 25. Local model output in wet season on the study area.	27
Figure 26. Local model output in dry season on the study area.	28
Figure 27. Monthly mean total alkalinity's estimations from local model output.	29
Figure 28. Temperature effect on seawater pH and Total Alkalinity.	30
Figure 29. Seawater dilution effect on chemical speciation.....	31
Figure 30. The increase of CO_2 concentration based on Mauna Loa Observatory(Scripps Institution of Oceanography, 2009).....	31
Figure 31. Yearly CO_2 increasing effect on the study area.	32
Figure 32. Monthly mean salinity and temperature variability in the study area.....	34
Figure 33. Indonesian Throughflow current.(Sprintall, Wijffels, Molcard, & Jaya, 2009).....	36

LIST OF TABLES

Table 1. Instruments list for in-situ measurement.....	10
Table 2. Seawater composition on salinity 35 PSu.....	14
Table 3. Nutrient concentration (gram/liter) on Nusa Penida seawater.....	14
Table 4. List of satellite for matchup.....	15
Table 5. Field measurement statistical analysis result.....	18
Table 6. Satellite data Match-up.....	19
Table 7. Charge balance error result from total alkalinity field measurement.....	20
Table 8. Output result from Aqion/Phreeqc on seawater od study area.....	21
Table 9. Model calibration and validation comparison between global and local model.....	24
Table 10. Monthly total alkalinity's standard deviation in the study area from local model output.....	29
Table 11. pH, Calcite, and Aragonite yearly decrease trend.....	32

ACRONYMS

TA	: Total Alkalinity
SST	: Sea Surface Temperature
SSS	: Sea Surface Salinity
WOA	: World Ocean Atlas
NOAA	: National Oceanic and Atmospheric Administration
AVHRR	: Advanced Very High Resolution Radiometer
Chl-a	: Chlorophyll-a
SPM	: Suspended Particulate Matter
CDOM	: Colored Dissolved Organic Matter
OLCI	: Ocean and Land Colour Instrument
NCEI	: National Centers for Environmental Information
SZA	: Solar Zenit Angle
ESA	: European Space Agency
SMOS	: Soil Moisture and Ocean Salinity
SSTA	: Sea Surface Total Alkalinity
ESA	: European Space Agency
SLSTR	: The Sea and Land Surface Temperature Radiometer
ARC	: ATSR Reprocessing for Climate
CMEMs	: Copernicus Marine Environment Monitoring Services
IDW	: Inverse Distance Weighted
CV	: Coefficient of Variation
RMSE	: Root Mean Square Error
CBE	: Charge Balance Error
EC	: Electric Conductivity
TDS	: Total Dissolve Solid
DIC	: Dissolve Inorganic Carbon
MAD	: Mean Absolute Difference
NaN	: Not a Number
ENSO	: El-Nino Southern Oscillation
NW	: North-West
SE	: South-East
MJO	: Madden-Julian Oscillation
ITF	: Indonesian Through Flow
OAPS	: Ocean Acidification Product Suite
IPCC	: Intergovernmental Panel on Climate Change
CTD	: Conductivity-Temperature-Depth (pressure)

1. INTRODUCTION

1.1. Background

In this century, the increasing carbon dioxide anthropogenic became an important issue. The environmental problems such as global warming and ocean acidification will emerge due to increasing of CO_2 . Oceans are known to act as a buffer in the ocean acidification. Around 30% of the atmospheric carbon in the air sank in the ocean (United Nations, 2015). This carbon sink will generate acidification in the ocean. Ocean acidification will change coral reef health and ecological condition (Soekarno, 1989). If this condition continues, the key marine organism such as fish and coral reef could diminish due to the difficulty to survive and sustain (Eisler, 2012). This is because all organisms in the ocean, from the smallest (plankton) to the largest, are very sensitive to small changes in pH levels.

We know that any decrease in pH leads to an increase in acidity. Ocean acidification is formed by CO_2 that is captured/absorbed on the sea surface reacts with seawater then form carbonic acid (H_2CO_3), thus reduce the pH level in seawater. However, this carbonic acid is unstable, they can turn into carbonate and bicarbonate ions in the sea water. This condition causes a decline in the growth of coral reefs and even further damages coral reef, because their ability to form calcium carbonate (CaCO_3) for their needs will disturbed (Eakin et al., 2010). The illustration of the ocean acidification process on the seawater can be seen in Figure 1.

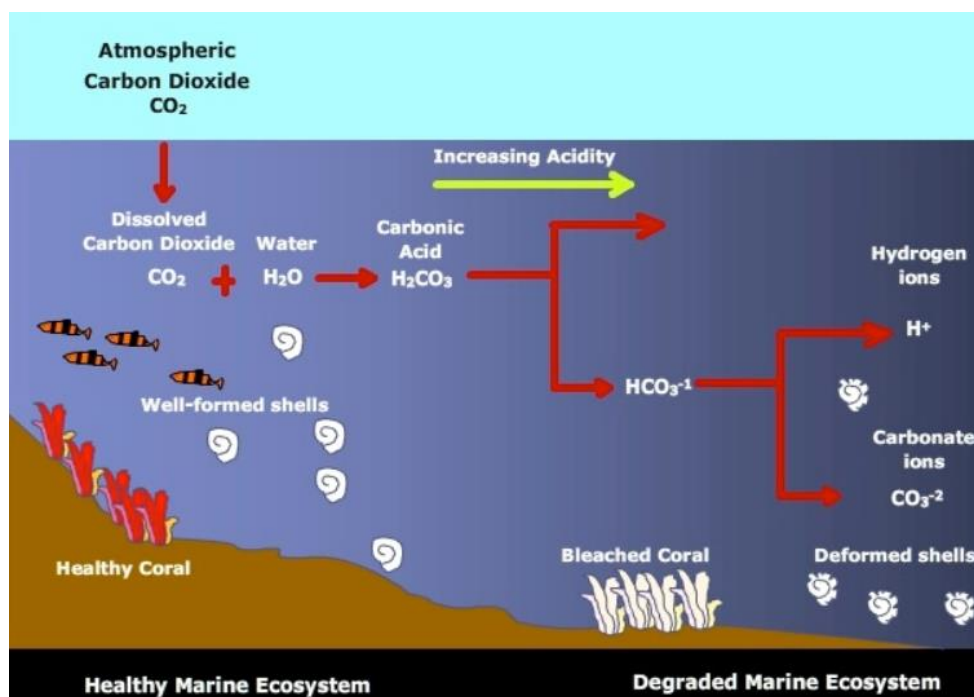
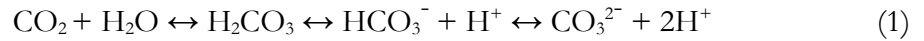


Figure 1. Ocean acidification process on the seawater (Ritter, 2016).

As a resume, the aquatic chemistry reaction for seawater acidification can be seen on the equation 1:



Seawater saturation state is important in biogeochemical equilibrium in the ocean. This carbonate saturation state consists of calcite and aragonite ion level. Calcite saturation more related to calcifying in the ocean, while aragonite saturation is a state of mineral carbonate equilibrium in the ocean. The seawater saturation state can give us the information regarding acidification in the ocean (GEOMAR Helmholtz Centre for Ocean Research Kiel, 2015). The equation for quantifying a saturation state is shown in the formula below.

$$\Omega = ([\text{Ca}^{2+}] \times [\text{CO}_3^{2-}]) / [\text{CaCO}_3] \quad (2)$$

The seawater saturation state can decrease because of ocean acidification, especially on aragonite saturation. If ocean pH decrease for 0.4, the carbonate ion will decrease approximately 50% on seawater (R. A. Feely et al., 2012). Furthermore, the aragonite saturation level will decline with respect to the decrease of the carbonate ion. Most marine organisms can live with aragonite conditions of more than 3. However, if the condition falls below 3, their lives will be disrupted (especially for organisms that require carbonate ions). Furthermore, if the saturation is below 1, they will disappear (NOAA, 2017a). In general, the aragonite saturation condition of the ocean in the world is supersaturated (around 4). However, for some regions, it has a low level of aragonite saturation. For instance, western arctic has aragonite saturation which varies between 0.9 – 1.2, and the southern ocean area around 1.3 – 1.5 (depending on the season) (Takahashi, Sutherland, Chipman, Goddard, & Ho, 2014). The Global aragonite saturation distribution can be seen in figure 2.

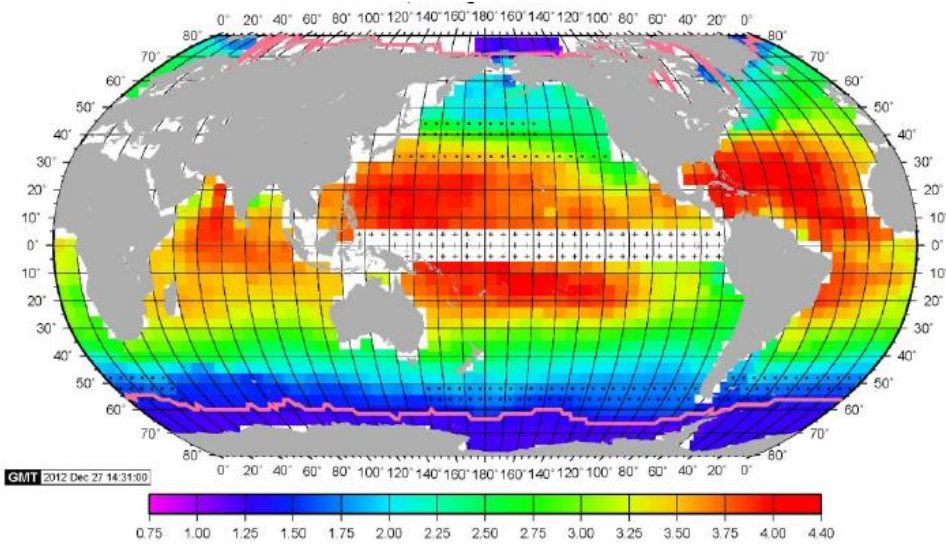


Figure 2. Global aragonite saturation distribution in August 2005. (Takahashi et al., 2014)

Aragonite saturation level on tropical area mostly in supersaturated condition (NOAA, 2014). If the aragonite condition in seawater is stay supersaturated, the ability of seawater to hold CO₂ in the ocean become maximum (IPCC, 2007). Ocean acidification can reduce this aragonite saturation state. Further, this aragonite state is related to the alkalinity. The additional acid will reduce the alkalinity in the seawater solution (Doney, Fabry, Feely, & Kleypas, 2009). According to Millero, the total alkalinity and pH doesn't have a direct relationship(Doney et al., 2009). However, there are some additional influences from carbonate ions (Frank J Millero, 1995). Further research is still needed to find out the relationship between the two. We can see the correlation between the total alkalinity and pH from equation 3.

$$TA = [HCO_3^-] + 2[CO_3^{2-}] + [B(OH)_4^-] + [OH^-] - [H^+] \quad (3)$$

According to NOAA (NOAA, 2017b), the global sea surface pH conditions nowadays is at level of 8.1 nowadays. Although a lot of CO₂ is absorbed by the oceans, it can still be buffered by the alkaline ions in the ocean (Dore, Lukas, Sadler, Church, & Karl, 2009).

It will be beneficially if the alkalinity levels are known by remote sensing globally. This will provide information about how far the ocean can survives from the acidity that occurred. Furthermore, the effect of the alkalinity level decreasing and ecology changing due to ocean acidification can be explained effectively and efficiently.

Satellite observation and in-situ measurements have their advantages and disadvantages respectively. On the one hand, several advantages of using remote sensing observation are synoptic coverage from local to global scales (high scale), frequent revisit time and extended time series (temporal scale), and the most important factor is low cost. On the other hand, remote sensing also has limitation, such as difficulty to directly measure and quantify acidification. In this case, model is needed for processing the data from satellite observation to quantify the acidification on the ocean. For example in this study, sea surface temperature (SST) and sea surface salinity (SSS) are the important parameters to be measured in observing the occurrence of the ocean's acidification (Eakin et al., 2010). For instance, Sentinel-3 can be used to observe sea surface temperature (SST) (ESA, 2018.-a) and SMOS to observe Salinity (SSS) (ESA, 2018.-b). Although in-situ measurements have low spatial resolution compared to the remote sensing observation, in-situ measurements are still used in the remote sensing observation to calibrate and validate the model (Yang, Liu, & Shan, 2013). The challenge is to integrate between the in-situ and the satellite observation. This combined approach can give the accurate information regarding ocean acidification and how it affects to the environmental in the ocean (Knudby, Pittman, Maina, & Rowlands, 2014).

1.2. Research Problem

Ocean acidification has become an important phenomenon nowadays. Hence, it would be useful if we can figure out the impact of the ocean acidification on the ecological parameters such as the concentration of Chlorophyll-a changes based on remote sensing observation. Further, the problem occurs because these phenomena cannot be observed directly from satellites. Therefore, we must use modelling approach.

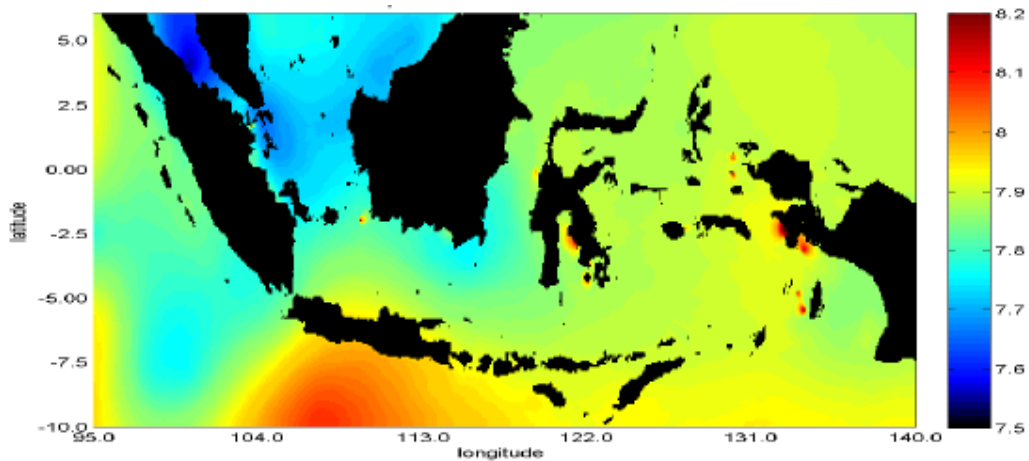


Figure 3. Average pH in the Indonesian ocean using Hamburg Shelf Ocean Model (HAMSO) for 1992-2009 (Putri, 2015).

Various studies have been conducted to analyse ocean acidification. However, their model approach is based on in-situ measurements. For example, there is a study of pH variations in the Indonesian ocean carried out by Indonesian researcher using the Hamburg Shelf Ocean Model. Their modelling approach used a database from the World Ocean Atlas 2009 (WOA 2009) for salinity and sea surface temperature as input parameters (Putri, 2015). World ocean atlas (WOA) is in-situ climatology measurement for several parameters such as temperature, salinity, dissolved oxygen, etc (N. N. C. for E. I. US Department of Commerce, 2017). Their research results depicted on figure 3.

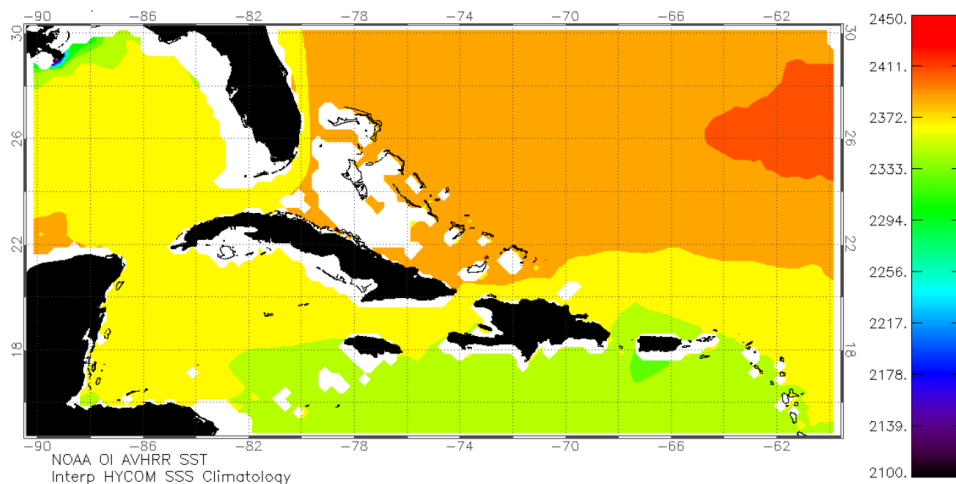


Figure 4. Experimental model for Total alkalinity concentration ($\mu\text{mol/kg}$) in Greater Caribbean Region on 2012 (NOAA, 2014).

Researcher at NOAA coral reef watch division observed the alkalinity level of the Great Caribbean Region since 2008. They applied the Lee's model for subtropics ocean on the Atlantic region to analyse the total alkalinity concentration in their study area. For the Input model parameters, they used the NOAA-AVHRR satellite data for SST and Real-Time Ocean Forecast System (Atlantic) for SSS data. The result of this modeling was then validated using in-situ measurements from geochemical cruise data sets by NOAA (Gledhill, Wanninkhof, & Eakin, 2009). The result of the analysis regarding this total alkalinity can be seen in figure 3 below, where the spatial resolution obtained is still rough, which is 0.25° or equivalent to 27 km.

The aim of this study is trying to quantify the ocean acidification in Indonesian ocean, particularly in Nusa Penida, Bali using earth observation data for 1 years. The study will generate local model based on global Sea Surface Total Alkalinity Model (Lee et al., 2006) where the sea surface salinity (SSS) as input parameters will be retrieved from SMOS satellite and the sea surface temperature (SST) will be retrieved from the Sentinel-3 satellite.

1.3. Justification

Monitoring acidification will help understanding the correlation between ocean acidification and ecological and its effect on aquatic environment. This study will help the stakeholder for mapping the vulnerable areas and determining the necessary mitigation criteria with regards the ocean acidification. Furthermore, stakeholder can take proper actions or make appropriate regulation to minimize the impact of ocean acidification on the area of their responsibility.

1.4. Research Objectives and Questions

1.4.1. General Objective

The general objective of this study is to quantify the total alkalinity in Nusa Penida, Bali, Indonesia using modelling.

1.4.2. Specific Objective

- To simulate the ocean acidification using remote sensing and aqua chemistry model.
- To generate a local sea surface Total Alkalinity model based on a global model of Lee et.al. (2006) for analyzing the ocean acidity and conditions based on total alkalinity around Nusa Penida, Bali.
- To map the total Alkalinity on Indonesian ocean water with finer spatial resolution.

1.4.3. Research Questions

- What is the ocean acidification condition in the study area based on remote sensing and aqua chemistry modelling?
- How temperature and salinity effect pH and total alkalinity on the study area?

1.5. Study Area

95 percent of coral in South-East Asia is highly vulnerable to bleaching due to ocean acidification. Indonesia, as one of the countries in South-East Asia, is one of coral reef triangle in the world which has a high diversity (Jennerjahn, 2012). According to Hedley, Indonesia together with Philippine have high coral reef coverage ($\pm 32.000 \text{ km}^2$) on their coastal area (Hedley et al., 2018). In Indonesia, Bali have good coral quality and coral cover. The study area is located on Badung strait, on Nusa Penida region, Eastern Bali, Indonesia. Geographically, Nusa Penida is located at $8^\circ 44' 49'' \text{ S}$ and $115^\circ 31' 56'' \text{ E}$.

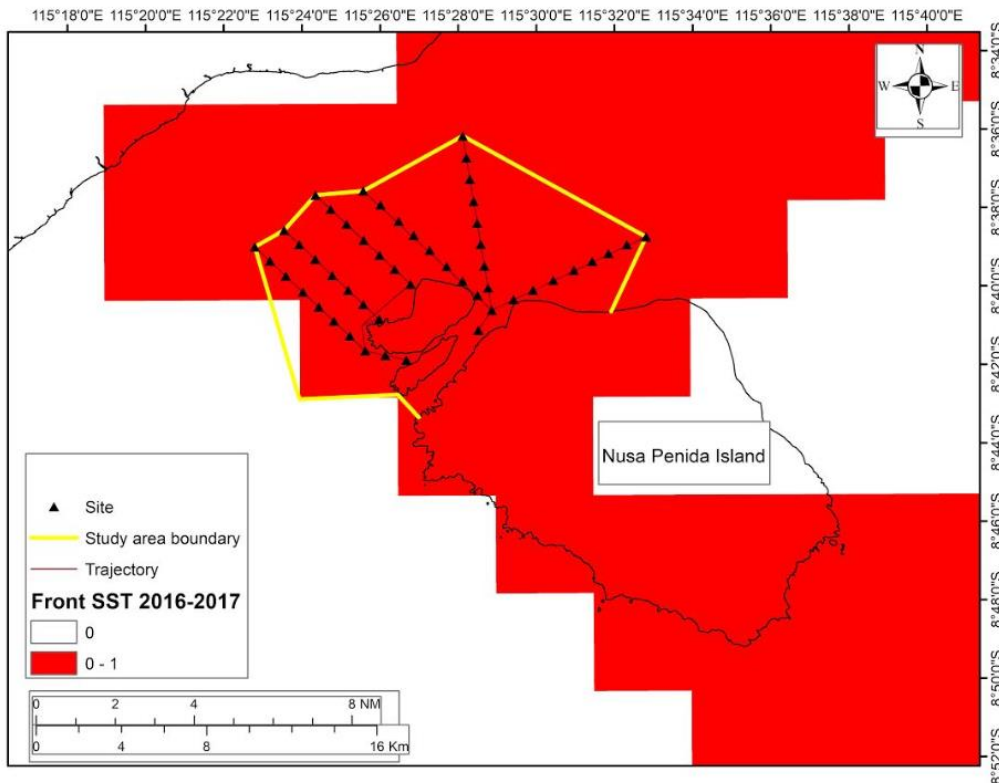


Figure 5. In-situ measurement trajectory.

The study area in this study can be seen in Figure 5, where the yellow line is the boundary of the study area. The study area is divided into 6 trajectories, where each route will be taken 2 times during fieldwork. This is because there are 12 times matchups between the in-situ measurements with Sentinel 3 during fieldwork (10 September to 15 October). We expect 1 trajectory will get 2 matchups with satellite observation. On one in-situ measurements trajectory, we will be divided by 10 sampling points, and several points have been measured more than 2 times. The distance of each point is 1 km, and approximately measurement time is 15 minutes for each point. The in-situ measurement was carried out from 09:00 until 13:00 local time. This is because, based on the calculation of the solar zenith angle (SZA) in the Nusa Penida, Bali on that time range is between 60° until 20° . In this SZA range good for matchup between in-situ measurements and satellite observations.

2. METHODOLOGY

2.1. Work Flow

Figure 6 describes a general methodology flowchart of this research to answer the research questions and obtain the desired objectives. The research is intended to quantify the total alkalinity concentration in Nusa Penida based on earth observation data by applying Lee's model (Lee et al., 2006).

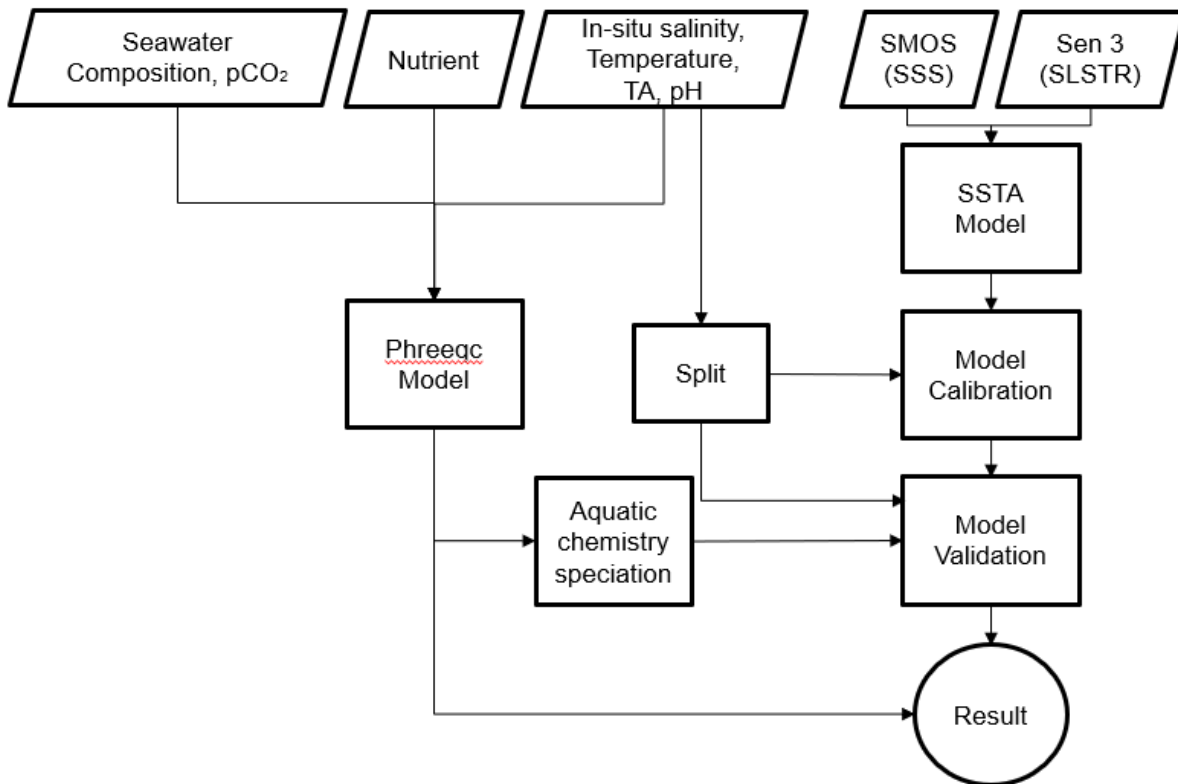


Figure 6. The flow chart of the methodology for the study.

2.2. Fieldwork

2.2.1. General Description

This research was carried out in Badung Strait, Bali, Indonesia. On the fieldwork, data measurement was divided into two periods. The first period was on 10 to 18 September 2018, and the second period was held on 6 to 15 October 2018. The study area consists of 6 trajectories. Each trajectory has 10 sampling point. Sampling points distribution that we observe is shown in Figure 7. The trajectory order from number 1 to number 6 respectively from right to left side. First sampling points measurement was noted by round dots, while the second measurement was noted by square dots. Garmin GPS MAP was used for sampling points marking. This sampling points marking was done after arriving at the target measurement location. The accuracy of the target sampling point with the actual point is less than 50 m.

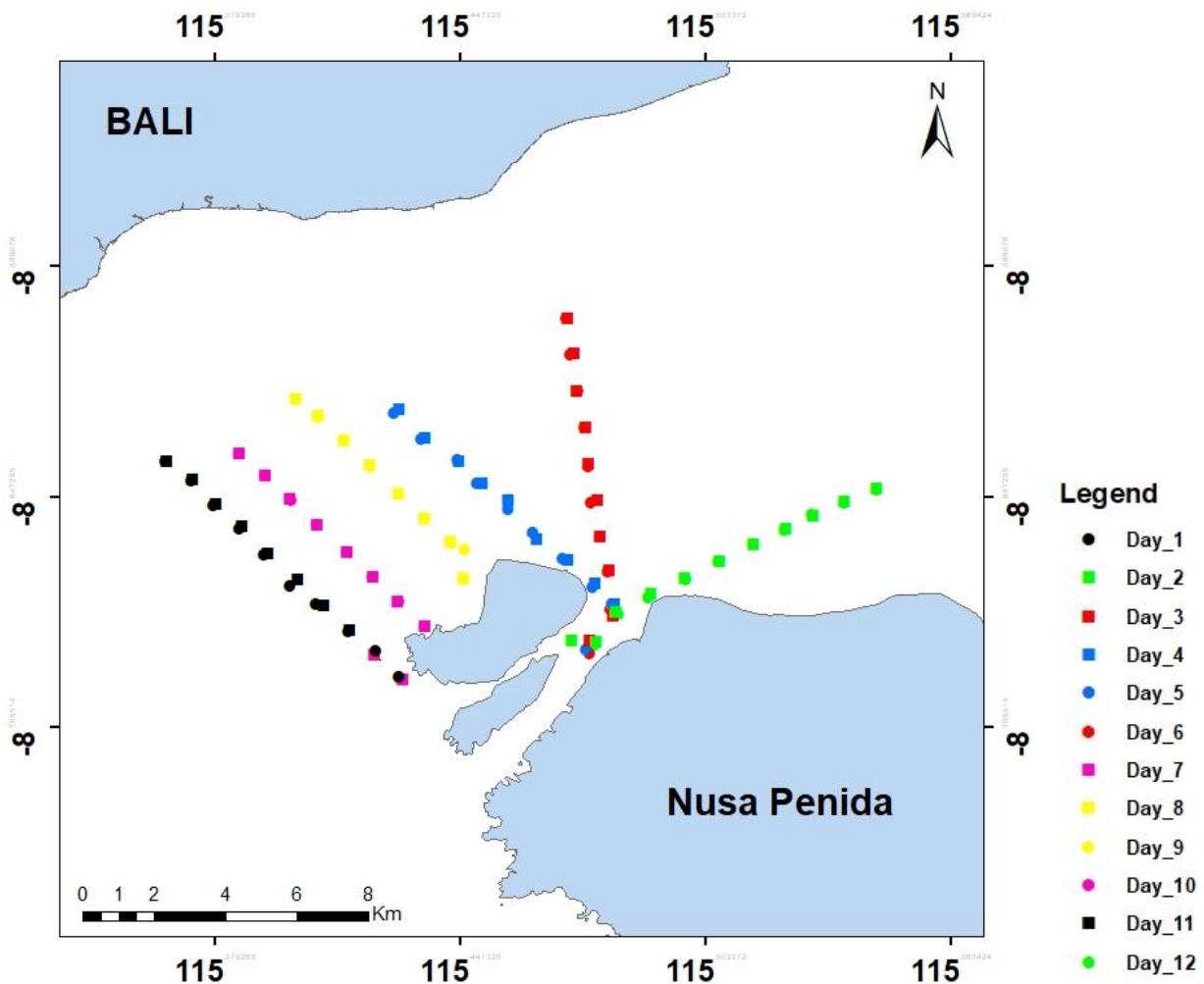


Figure 7. Sampling point on this research

2.2.2. Measurement Procedure

Firstly, all the instrumentation used for in-situ measurement, except the echo sounder, was assembled when the boat was still on the harbour. The echo sounder instrument (fish detector) was mounted on the boat side at the first sampling point for time saving reason. This was done because when the eco sounder device was installed, the boat speed becomes very limited, which is less than 6 knots.

After reaching the first sampling point, firstly the actual sampling point was marked using GPS. In addition, the fish and bathymetry data were taken by using eco sounders. Then the water quality was measured using the WQC-TOA DKK instrument for pH, temperature, salinity, and chlorophyll parameters at the sampling location. The next step was taking a radiometer measurement using Trios Ramses. The last step was taking seawater sampling using bottle for alkalinity measurements. Specifically, the alkalinity analysis was carried out shortly after arriving on land using AquaMERCK 111109.0001 by titration method. All these measurements were carried out with less than 5 minutes. Figure 8 and 9 illustrates our measurement process.

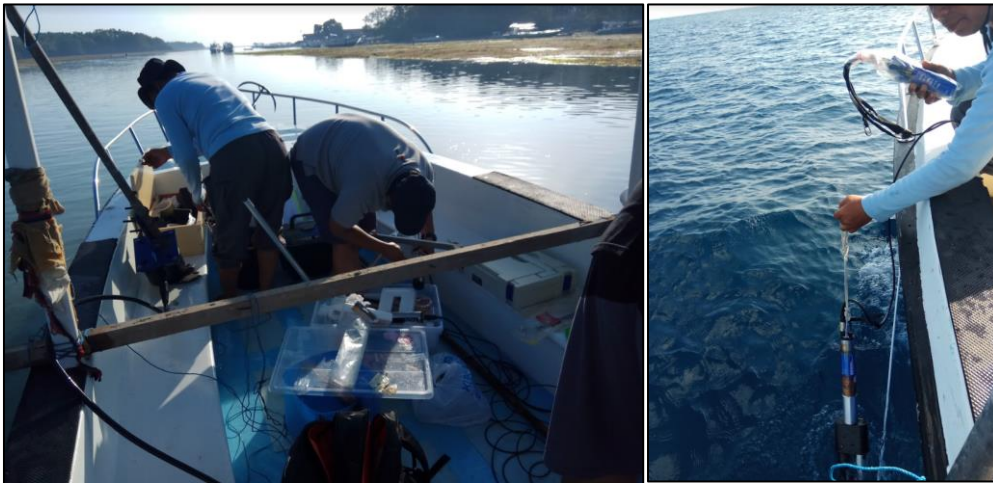


Figure 8. Instrument preparation (left) and WQC-TOA DKK measurement (right).



Figure 9. Seawater sampling (left) and Total Alkalinity measurement (right).

2.2.3. In-Situ Measurement

Table 1. Instruments list for in-situ measurement.

Equipment	Dataset	Unit
Trios Ramses	Radiometer	Nm (Nano Meter)
Garmin GPSMap	Sampling point coordinate	-
Aquamerck 1.11109.0001	Alkalinity	mmol/l
TOA-DKK WQC 24	Salinity	PSu
	Seawater temperature	°C
	Chlorophyll	µg/l
	pH	-

The in-situ data will be used to analyse the accuracy of the calculations obtained from the model. 120 samples were taken from in-situ measurement, obtained from 10 sample points from each trajectory. In-situ measurements were taken from the boat operating in accordance with the satellite pass schedule. Hence, the matchup between in-situ sampling data with satellite dataset has to be done on the same location at the same time over the study area. In-situ measurement was taken several data such as radiometer, bathymetry, salinity, sea temperature, and chlorophyll. Instrumentation details for in-situ measurement, can be seen on the table 1.



Figure 10. Instrument used for field measurement in this research are TOA-DKK WQC 24 (left), Garmin GPSMAP sounder (middle) and Trios Ramses (Right).

pH measurement

The TOA-WQC DKK 24 instrument was used in this in-situ measurement. In this measurement we found that the overall pH value in the study area was high. This is because the observations were done in the dry season where the seawater temperature is high. This is in line with the results of research from BROL which states that low temperatures will increase dissolved CO₂ and will reduce pH (Triyulianti, Widagti, Rintika, & Tenggono, 2012). In addition, according to Safitri research, the highest pH in the Balinese sea occurs around September (Safitri & Putri, 2009).

The results from pH in-situ measurements can be seen in the figure 11. The pH value in the study area varies from 8.11 to 8.43, with an average 8.28. The average pH of this in situ measurement is high (more than 8.2). According to Milerio, the average pH of the seawater is around 8.2 (Frank J Millero, 1995).

The lowest pH (8.11) was found in point 3 on trajectory number 4 in the day 9 measurement. The highest pH value was found in point 3 on trajectory number 1 in the day 12 measurement. The standard deviation for this pH measurement is less than 0.075.

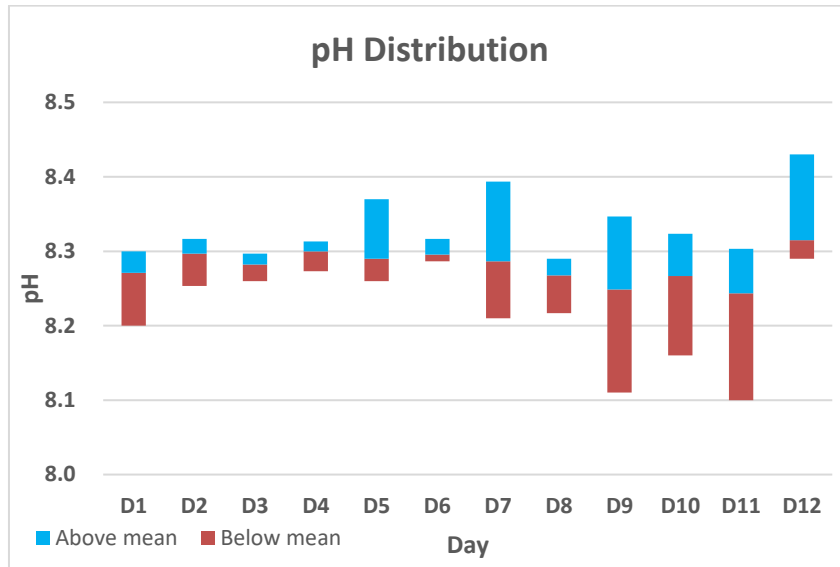


Figure 11. pH field measurement distribution.

Alkalinity measurement

On average, our in-situ alkalinity measurement results relatively high. The values vary from 1.9 mmol/liter to 2.6 mmol/liter. The average result, is 2.3 mmol/liter, is higher than Lee's model prediction that the alkalinity in the equator ranges around 2.29 mmol/liter. This is due to the high temperature and salinity conditions in the dry season. These two parameters are important factors that cause high values of alkalinity of seawater in our study area, especially in the Badung Strait of Bali.

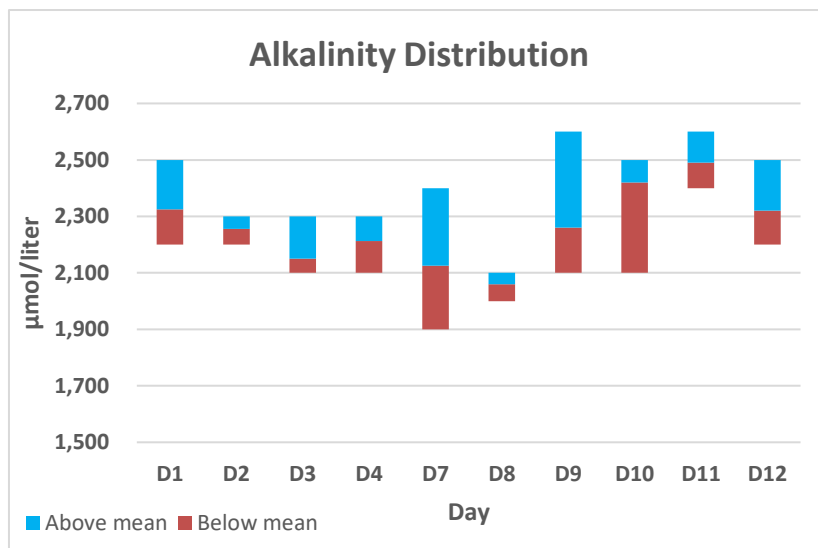


Figure 12. Total alkalinity field measurement distribution.

In this alkalinity in-situ measurement, the lowest alkalinity value (1.9 mmol/liter) was found in the 9th day measurement on trajectory number 5 at point 9. While the highest alkalinity value (2.6 mmol/liter) was found in measurements of days 9 and 11. The standard deviation in this field measurement is less than 0.167.

Salinity measurement

The salinity measurements in this study area was used the TOA-WQC DKK instrument. However, due to the obstacles in the salinity sensor, the measurements from day 7 to day 10 used a refractometer and on day 11 until 12 use both instruments. We can see from the figure 13, between refractometer and TOA-WQC DKK have close measurement result on day 11 and 12. The salinity mean measurement on TOA-WQC on day 11 (33.7 PSu) and day 12 (33.9 PSu) are close to refractometer measurement which is 34 PSu. However, the refractometer precision is less then TOA-WQC sensor because the refractometer cannot measure the value below decimal.

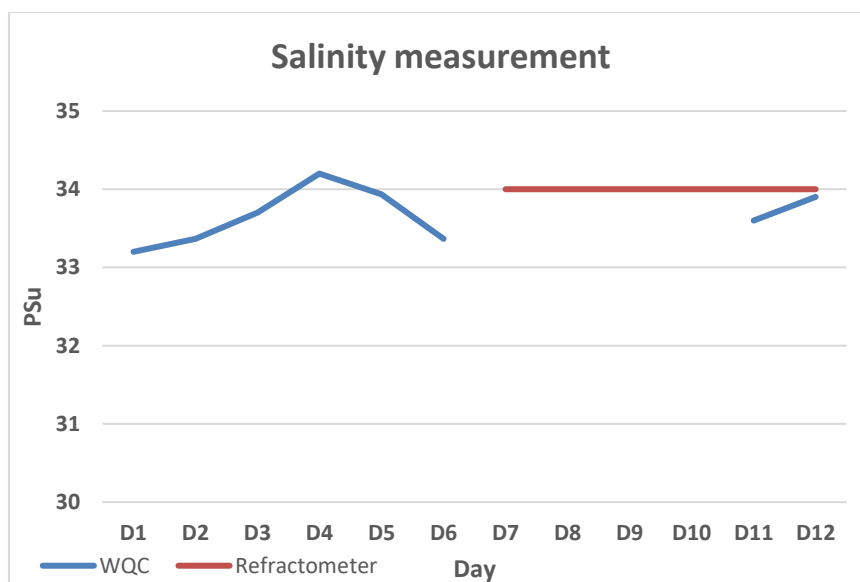


Figure 13. Salinity consistency measurement between WQC and refractometer.

The measured salinity values in the study area was vary from 33.2 to 34.3 PSu. Salinity values in this study area are high. The highest salinity of the Indonesian sea occurs around September, on the peak of dry season, and the lowest occurs around May on the rainy season (Najid, Pariwono, Bengen, Nurhakim, & Atmadipoera, 2012). However, the value of salinity in Indonesia has seasonal variability (seasonal changes). In the in-situ measurements, we found the lowest salinity value (33.2) occur on the 1st day measurement on trajectory number 6 at point 1. And the highest salinity value was found on days 3, 4, 11 and 12 measurements. The standard deviation of this field measurement is less than 0.388.

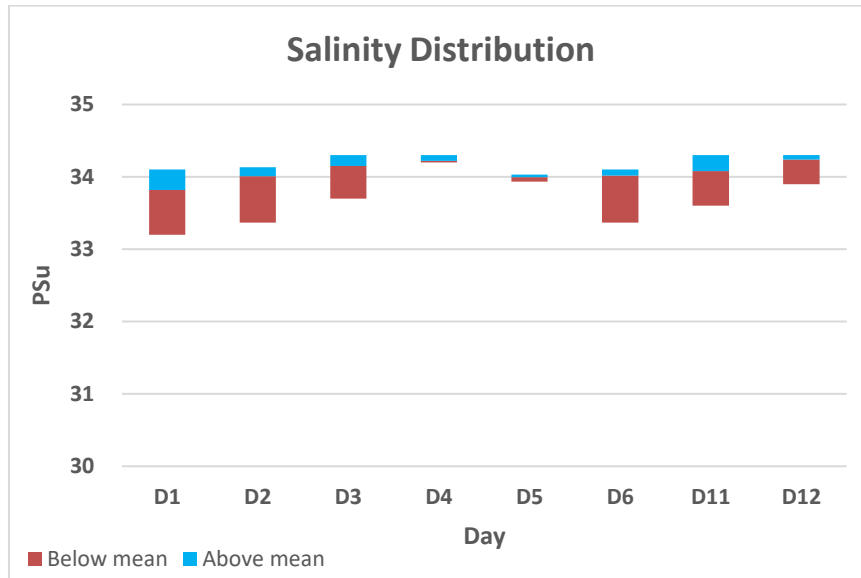


Figure 14. Salinity field measurement distribution.

Temperature measurement

The TOA-WQC DKK instrument was used to measure the temperature. In this in-situ measurement, the temperature values obtained are varied from 19.2°C to 28.5°C. This large measurement range/variation was obtained because the measurements were done in the morning until noon. This can be seen from the value of the temperature which was initially low at point one then increased to point number 10. On the dry season, the peak of the sea temperature can vary from 28 °C to 30 °C. The sea surface temperature on September and October 2018 are high because these months are still in the dry season of 2018 which starts from April 2018 and the peak is on September (BMKG, 2018).

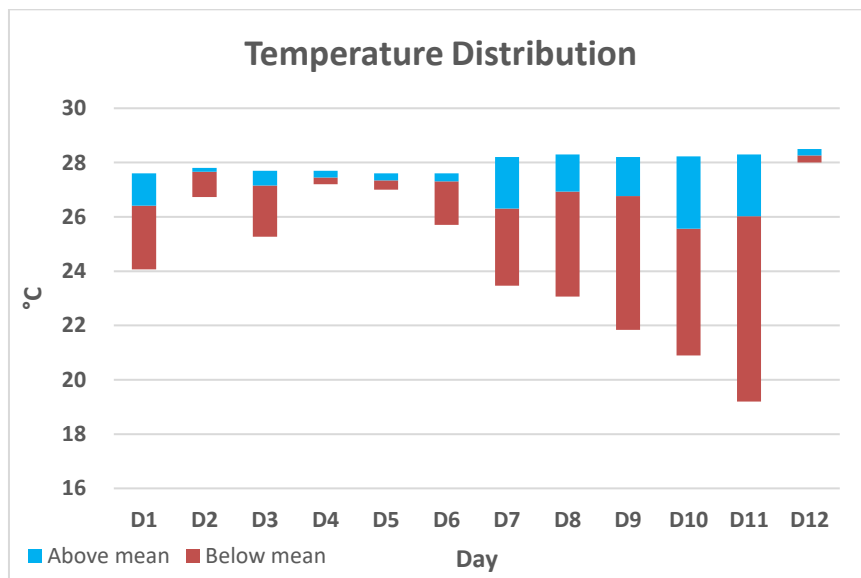


Figure 15. Field measurement of temperature distribution.

The average of sea surface temperature in this measurement is 26.9 °C. The lowest sea surface temperature (19.2 °C) was found in the measurement of day 11 on trajectory number 6 at point 2. The highest sea surface temperature was found in measurements of day 12 on trajectory number 1 at point 10. The standard deviation in this sea surface temperature measurement is less than 3.59. the temperature measurement variability on day 7 until 11 is high due to low temperature measurement on the beginning (morning).

Nutrient and Seawater composition

Table 2. Seawater composition on salinity 35 PSu.

Solute	mol
Na ⁺	0.46900
Mg ²⁺	0.05282
Ca ²⁺	0.01028
K ⁺	0.01021
Sr ²⁺	0.00009
Cl ⁻	0.54588
SO ₄ ²⁻	0.02823
HCO ₃ ⁻	0.00186
Br ⁻	0.00084
CO ₃ ²⁻	0.00019
B(OH) ₄ ⁻	0.00008
F ⁻	0.00007
B(OH) ₃	0.00033

Source: (F. J. Millero & Leung, 1978)

Nutrient and seawater composition are needed for running the Aqion / Phreeqc model. The seawater composition was taken from reference on salinity 35 PSu (F. J. Millero & Leung, 1978). While the nutrient composition was obtained from Marine Research and Observation Center (BROL), The Ministry of Marine and Fishery. The sample was taken on the first week of October 2018 on two location of the study area (mangrove point and crystal bay). The nutrient composition can be seen on the table 3.

Table 3. Nutrient concentration (gram/liter) on Nusa Penida seawater.

Location	Nitrat	Silika	Nitrit	Fosfat	Amonia
Mangrove point	0.034	0.419	< 0.002	< 0.002	< 0.006
Crystal Bay	0.063	0.311	< 0.002	< 0.002	< 0.006
Average	0.0485	0.365	< 0.002	< 0.002	< 0.006

2.3. Remote Sensing Data

2.3.1. General Description

Satellites observation that have been used in this research are Sentinel 3 and CMEMs (SMOS level 4). These satellites are owned by ESA (European Space Agency) to support their mission regarding Global Monitoring for Environmental and Security (ESA, 2018a). Sentinel satellite has several advantages, such as good spatial and temporal resolution. The SMOS (Soil Moisture and Ocean Salinity) satellite is an ESA satellite specifically designed to monitor soil surface moisture and sea surface salinity globally. The detailed information about the satellites that will be used can be seen in the table 4.

Table 4. List of satellite for matchup.

Satellite	Spatial Resolution	Temporal Resolution	Size	Format
Sentinel 3 (SLSTR)	0.5 Km	1 Day	100 MB	NC
SMOS (L4)	15 Km	3 Days	7 MB	NC

2.3.2. Reprocessing Satellite Data

Sea surface temperature

In this study, sea surface temperature data was retrieved from Sentinel 3 SLSTR. Actually, during the fieldwork, Sentinel 3 was passing 11 times on our study area. However, from 11 times Sentinel 3 passed, there were only 8 days that had SLSTR data, the remaining 3 days only had OLCI data. In this study, the data used came from Level 1 product then processed using SNAP software to get sea surface temperature data.

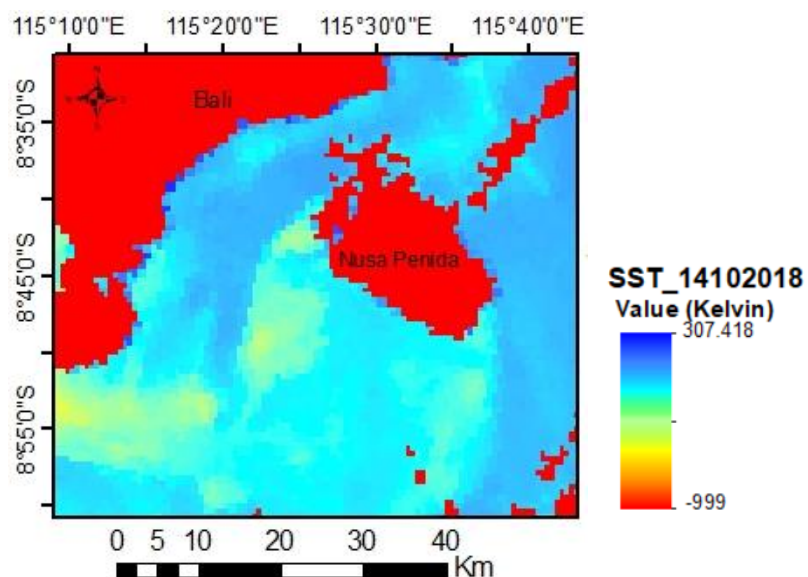


Figure 16. Sentinel 3 ARC SST data product at 14 October 2018.

In the data reprocessing, first, re-projecting the level 1 SLSTR product data from Sentinel 3 that has been downloaded. Reprojection was done to change the coordinate system on the image into the WGS 1984 coordinate system. Then the subset process was done for image from Sentinel 3 focused only in the study area. Furthermore, processing level 1 data into temperature data using the ARC toolbox at SNAP. For instance, the product from ARC-SST toolbox can be seen on figure 16. Then extracting the value from the raster image correspond to the sampling point in in-situ measurement. However, there are several sampling points that do not have temperature data due to cloud cover.

Sea surface salinity

In this research, the sea surface salinity products from SMOS satellites was used to get salinity from remote sensing data. During the fieldwork, there were only 5 times SMOS satellite passing on the study area (ascending and descending). Although the data used was a level 2 product from SMOS, the salinity data cannot be used directly due to the absence of salinity data on the study area. This is because the study area in the Badung Strait of Bali is flanked by the main islands (Bali) and Lembongan which is close to the land value.

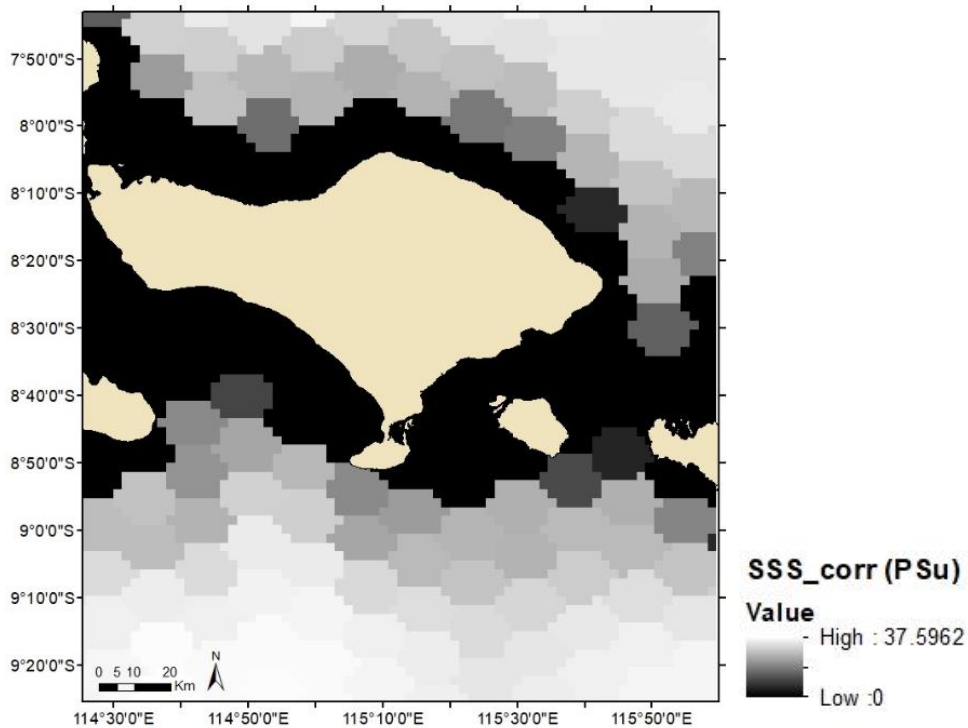


Figure 17. SMOS salinity (level 2) data on 15 October 2018.

Therefore, this research uses the higher salinity product level from CMEMs (Copernicus Marine Environment Monitoring Services). They provide daily until monthly composite data of Sea Surface Salinity Level 4 based on SMOS satellite (Copernicus, 2012). They fill the NaN (Not a Number) data using the interpolation from combination between SMOS data, salinity in-situ data, dan SST (sea surface

temperature) dataset (Nardelli, 2012). Further, this CMEMs-SMOS data was processed in the Map Arc to do the resample and interpolation process. The Resample aim is to change the pixel size from 10 km to 500 meters. The interpolation method used is inverse distance weighted (IDW) to fill the the mixing pixel near the land value. For instance, the interpolation results on salinity data from CMEMs-SMOS can be seen in the figure 18. The salinity in study area obtained from this data close to the in-situ measurement. During the fieldwork, CMEMS Salinity values vary from 33.88 PSu to 34.34 PSu.

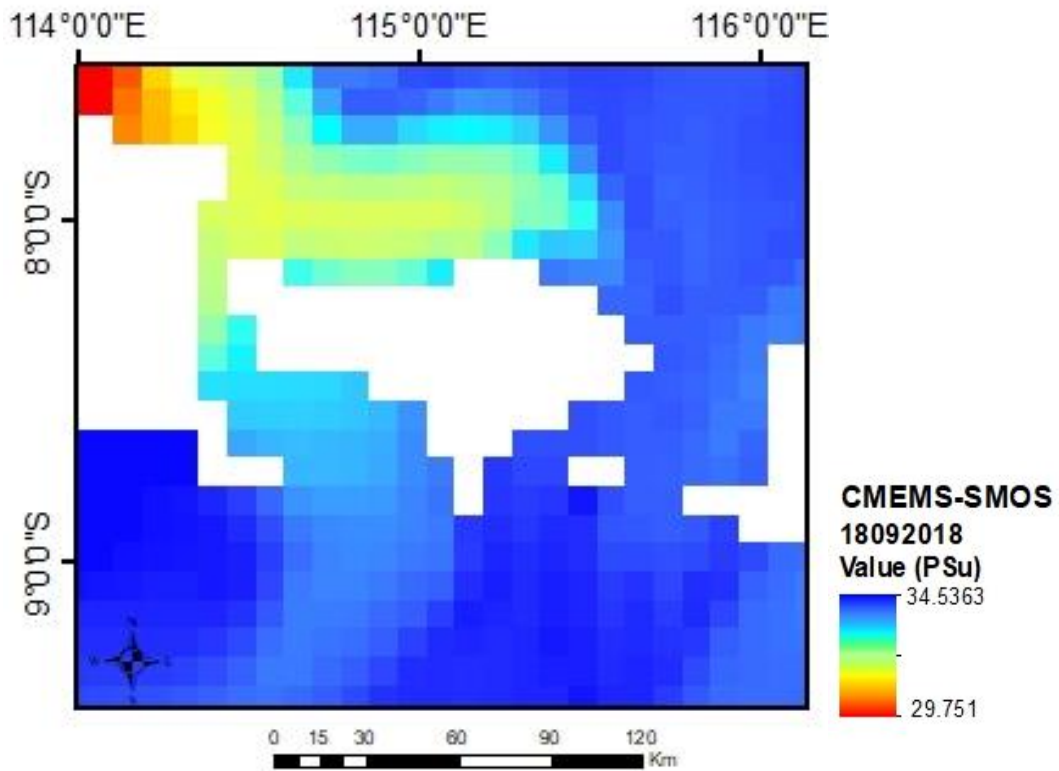


Figure 18. CMEMs salinity (SMOS level 4) product.

3. ANALYSIS

3.1. Fieldwork Data Analysis

Table 5. Field measurement statistical analysis result.

	pH	Alkalinity (mmol/liter)	Salinity (PSu)	Temperature (°C)
Min	8.1	1.9	33.2	19.2
Max	8.43	2.6	34.3	28.5
Mean	8.28	2.26	34.04	26.93
Median	8.29	2.3	34	27.6
St. Dev	0.046	0.164	0.2	1.873
D.Range	0.33	0.7	1.1	9.3
CV	0.01	0.07	0.01	0.07
CV1	0.039	0.309	0.032	0.345

From the field data that has been obtained, a statistical analysis such as standard deviation, minimum and maximum values, dynamic range, mean, coefficient of variation was calculated. Standard deviation is the statistical value used to determine how the data is distributed in the sample, and how close the individual data points are to the mean (average) of the sample. If the standard deviation value close to 0, then the sample distribution is relatively the same and close to the mean value. We can see the results of the calculation of the standard deviation on 5 parameters from the field measurement datasets, only the temperature which has a value far from 0. This is due to the long measurement range (± 3 hours), where the temperature changes very easily within the measurement range.

Dynamic range is the range of samples (differences) from the smallest (minimum) measurement values with the largest value (maximum). The largest dynamic range value from the five parameters is in the temperature measurement (9.3). Then, we analyse the coefficient of variation from the five parameters. The variation coefficient can be used to determine the ratio from our data distribution with mean value, so we can know how vary our data is. From the five parameters, only chlorophyll which has the largest CV value.

Furthermore, we analyze the field measurement data using histogram analysis to see where the outliers from each parameter. Based on this analysis, from the five parameters, only the alkalinity measurement which does not have outlier. We can see from figure 19, on alkalinity histogram, there is no point below the minimum and above the maximum value limit. Then, we analyze the location where this outlier occurs. From these four parameters, mostly all the outlier occurs in the first measurement to the third measurement every day, except the measurement of day fourth (does not have outliers).

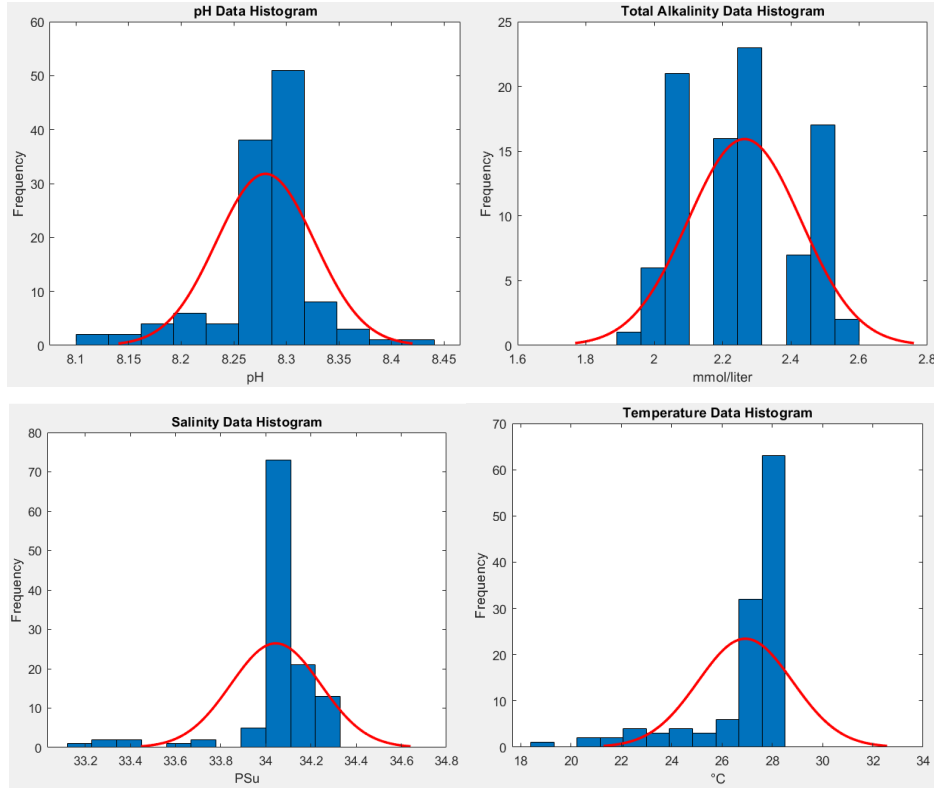


Figure 19. Histogram analysis on each parameter.

3.2. Satellite Data Analysis

Table 6. Satellite data Match-up.

Satellite	Parameter	R ²	RMSE	Unit
Sentinel 3 (SLSTR)	Temperature	0.29	2.76	°C
CMEMS	Salinity	0.19	0.15	PSu

On the temperature validation part, the research use sea surface temperature product from Sentinel 3 compared with the in-situ datasets. The aim of this validation is to measure the RMSE and R² from the retrieval. The RMSE result from temperature retrieval is 2.76 °C. The temperature obtained from Sentinel 3 varies from 26°C to 28.5°C. The average sea surface temperature obtained is 27.8°C. While for salinity satellite data validation, salinity data from SMOS satellite level 4 (CMEMS) result compared with the salinity in-situ dataset. From the validation, the RMSE value of the salinity retrieval is 0.15 PSu, with RMSE 0.15 PSu.

The results from satellite data validation show that even though the resulting error (RMSE) is small, the R² value obtained is also small. This small R² is caused by a bias between satellite measurements and in-situ measurements. This bias arises because of the difference in spatial scale between the satellite measurements and the field measurements (Allard, D.; Baret, F.; Weiss, 2006). Furthermore, bias in salinity measurement using CMEMS may arise because optimal interpolation results (OI) do not work well in coastal areas that have complex topography (Nardelli, 2012).

3.3. Aquatic Chemistry Validation Using Aqion/Phreeqc

Aqion software is hydrochemistry and water analysis modelling that uses the Phreeqc software in it as a USGS numeric solver. This software was developed by Harald Kalka, a practitioner of environmental chemistry from UTT Dresden Germany. One of the uses of Aqion is to validate aqueous solutions using CBE (charge balance error) or EC (electric conductivity) (Aqion, 2012) . On this research, CBE used for validating the alkalinity dataset from in-situ measurement and also validating the total alkalinity calculation from remote sensing model.

On water sample data validation, first enter the composition of the seawater sample. At this stage, we can enter key parameters such as pH, temperature, alkalinity from field measurements. Next, we need to enter the concentration of each element forming a solution of sea water and nutrients such as Ca, Mg, Na, K, etc. Then, we run the software for calculating the CBE (Charge Balance Error) on the solution. The following table are the results of a charge balance error analysis on field measurement dataset.

Table 7. Charge balance error result from total alkalinity field measurement.

Alkalinity (mmol/liter)	CBE (%)
1.9	0.03
2	0.02
2.1	0.01
2.2	0
2.3	0
2.4	0.01
2.5	0.02
2.6	0.03

The largest CBE is found in alkalinity values below 2 mmol/liter and above 2.5 mmol/liter. The accepted CBE value is under 0.03% based on aqua chemistry analysis from Aqion software. Therefore, can be concluded that good in-situ alkalinity datasets are in the range 2 mmol/liter to 2.5 mmol/liter. This validation in the alkalinity dataset can be used to determine which alkalinity value have un-balance chemical reaction. This is because, this in-situ alkalinity value will be used to validate and calibrate the local model that will be created. Moreover, the good alkalinity dataset can produce a good local model and reduce the errors that will arise later.

Using the hydrogeochemical model, we tried to analyze the water speciation in this study. The parameter inputs used such as seawater composition and nutrient concentration are from tables 2 and 3 in the previous chapter (chapter 2). Whereas pH and temperature used on calculation are the mean measurement in October. The results of the analysis using Aqion / Phreeqc model can be seen in table 8. Aragonite and calcite conditions on the study area are still super saturated (> 3).

Table 8. Output result from Aqion/Phreeqc on seawater of study area.

Water Speciation		Unit
pH	8.21	
Temperature	26.6	°C
pe	9.75	
CO ₂	3.41	pCO ₂
EC_25	51275	μS/cm
TDS	35.138	gr/L
Total Alkalinity	2.26	mmol/liter
DIC	1.98	mmol/liter
Ω Aragonite	0.56	*SI
	3.63	*CaCO ₃
Ω Calcite	0.703	*SI
	5.04	*CaCO ₃

3.4. Total Alkalinity Model Calibration and Validation

As a background on this study, we use Lee's the global Total Alkalinity model to estimate the ocean acidification level that occurs within the study area. The model algorithm with the second order polynomial form is used for the subtropics region, as shown in the equation below:

$$A_T = 2305 + 58.66 (SSS - 35) + 2.32 (SSS - 35)^2 - 1.41(SST - 20) + 0.040(SST - 20)^2 \quad (4)$$

Where: A_T = Total alkalinity (μmol/kg)

SSS = Sea surface salinity

SST = Sea surface temperature (°C)

In this study, to get a better spatial resolution on total alkalinity retrieval by Lee's model, we will use the data from Sentinel 3 and CMEMs (SMOS) satellite observation. Then, we will use the SMOS satellite to obtain sea surface salinity data. SMOS is a satellite of one of the ESA (European Space Agency) missions which aims to observe soil moisture and ocean salinity globally. SMOS has spatial resolution between 15-50 km depending on product level, and has 3 days temporal resolution (ESA, 2018c). Furthermore, for sea surface temperature data input, we will use Sentinel 3 (Sea Land Surface Temperature Radiometer) with 500 meter spatial resolution (reduced resolution) and 1 day temporal resolution (ESA, 2018b).

In this study, the Global Total Alkalinity Model was run using data sets obtained from field measurements (salinity and temperature). Furthermore, the results of this total alkalinity modelling are compared with the field alkalinity datasets. This was done to find out the errors generated by this global model. From the validation results, the RMSE produced by this global model is quite high, around 129.34 μmol / liter. This error is far from Lee's estimation that errors may occur around ± 8.1 μmol/liter (Lee et al., 2006). This high error model by Lee occurred since a global model works well in open ocean areas. Lee builds his model global total alkalinity model using datasets from the open ocean. The model will have a

different performance if used in coastal areas. Open oceans have a relatively stable biogeochemistry compared to coastal areas. This is related to biogeochemical changes in coastal areas affected by additional fresh water from lands (Land et al., 2015).

Local Model

In building the local model for sea surface total alkalinity, we used the global model from Lee model to be calibrated and validated using datasets (salinity, temperature, and alkalinity) from the field measurements. From the 120 measurement datasets that we have, we then removed the outliers (which were obtained from histogram analysis). Further, the alkalinity data is analysed by CBE to estimate which datasets have a low reaction error (CBE). As the result, 45 good datasets were obtained. These validation datasets were done to obtain a better local model that has low error.

Satellite based algorithm need to be calibrated and validated by in-situ measurement data (Land et al., 2015). The calibration and validation process were done using GeoCalVal method. The Calibration and Validation of geophysical observation models (GeoCalVal) method gives better model error and accuracy estimation on geophysical parameter (Salama et al., 2012). In this method, 45 datasets were sorted from low to high based on alkalinity values. Furthermore, these data were ordered in odd and even datasets. Odd datasets were used for calibration, while even datasets were used to validate the results of model calculations.

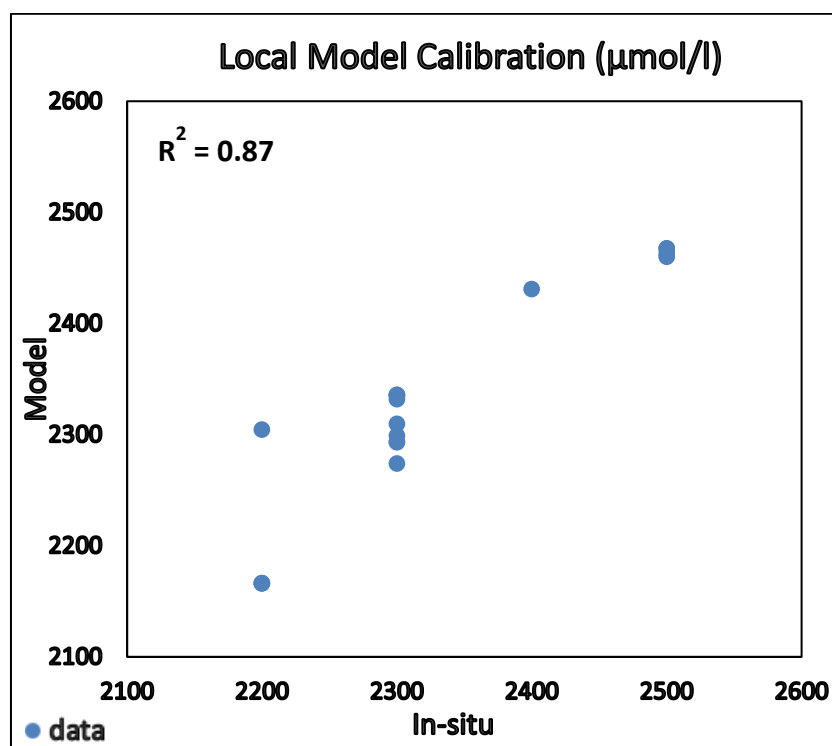


Figure 20. Local model calibration result.

In calibration, we tried to find 5 variables (a, b, c, d, e) that build up the local model of the total alkalinity (fitting). In determining these variables, the model fitting was done by the total alkalinity datasets from field measurements using the input parameters (salinity and temperature) at the same location. The local model obtained for the sea surface total alkalinity shown in the equation 5.

$$A_T = 1702 + (110.87 (SSS - 35) - 1026 (SSS - 35)^2) \times 0.8 + (1307 (SST - 20) - 68.25 (SST - 20)^2) \times 0.2 \quad (5)$$

Furthermore, in the validation process, the local total alkalinity model above to be run using an even dataset (salinity and temperature). Then the local model calculation results are compared with the field alkalinity value from an even dataset. The validation and calibration results were evaluated based on the RMSE, MAD and R^2 . The calibration and validation result can be seen on figure 20 and 21. The calibration and validation have good R^2 , because the R^2 value are close to 1. The coefficient of determination (R^2) of the local model is 0.87 for the calibration and 0.85 for the validation. The RMSE (root mean square error) from the calibration is 38.04 $\mu\text{mol/liter}$ and 42.95 $\mu\text{mol/liter}$ for the validation. The calibration and validation results can be seen in table 9.

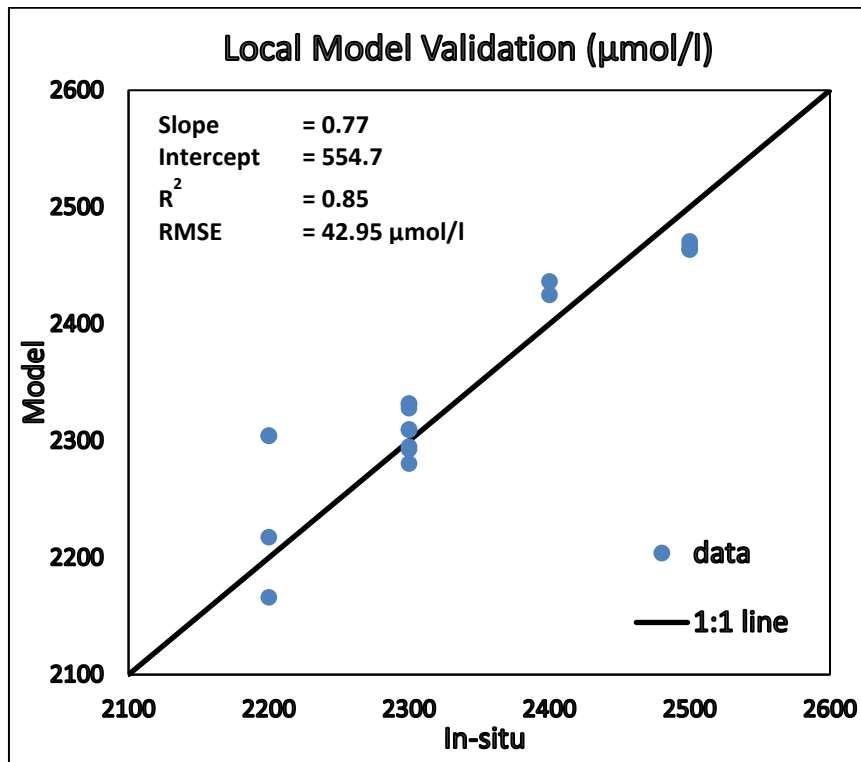


Figure 21. Local model validation result.

Table 9. Model calibration and validation comparison between global and local model.

Model Cal-Val	RMSE ($\mu\text{mol/liter}$)	MAD ($\mu\text{mol/liter}$)	R ²
Local model calibration	38.04	31.51	0.87
Local model validation	42.95	33.22	0.85

Figure 22 depicted the local model of total alkalinity performance on temperature 1°C - 36 °C and salinity 1 PSu - 41 PSu. We can see from the simulation that this local model of total alkalinity still sensitive on salinity changes. The total alkalinity increases along with salinity increase, however, after the salinity value 36 PSu, the alkalinity will decrease on increasing salinity. Although the local model is very sensitive in salinity, but also still sensitive on the temperature parameter changes (if we compare with the global model). The total alkalinity model will decrease until temperature 22°C, after that the total alkalinity will increase with increasing temperature.

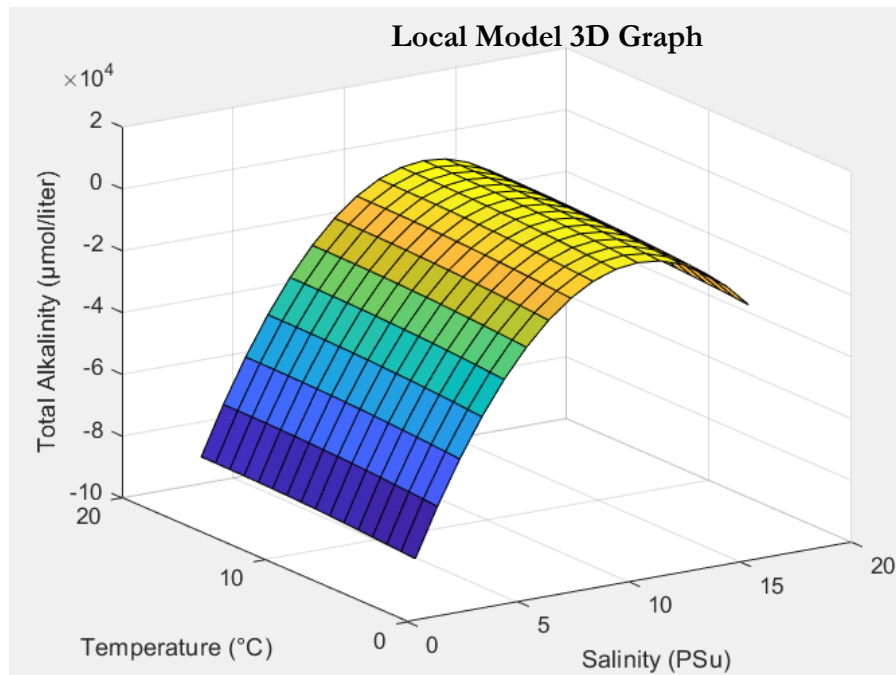


Figure 22. Local model assessment.

4. RESULT AND DISCUSSION

4.1. Result

4.1.1. Remote Sensing Modelling Result

The local model of total alkalinity from the chapter 3, was applied to the satellite data that has been processed. The CMEMs data were used as salinity data inputs while the Sentinel 3 (SLSTR) data were used as temperature data inputs. The total alkalinity estimation of the study area which used the satellite data can be seen in figure 23. The local model total alkalinity output results range from 1900 to 2593 $\mu\text{mol/liter}$ with 500 meter pixel resolution. The very small value in this total alkalinity mapping occurs due to the land pixel effect that has low salinity value.

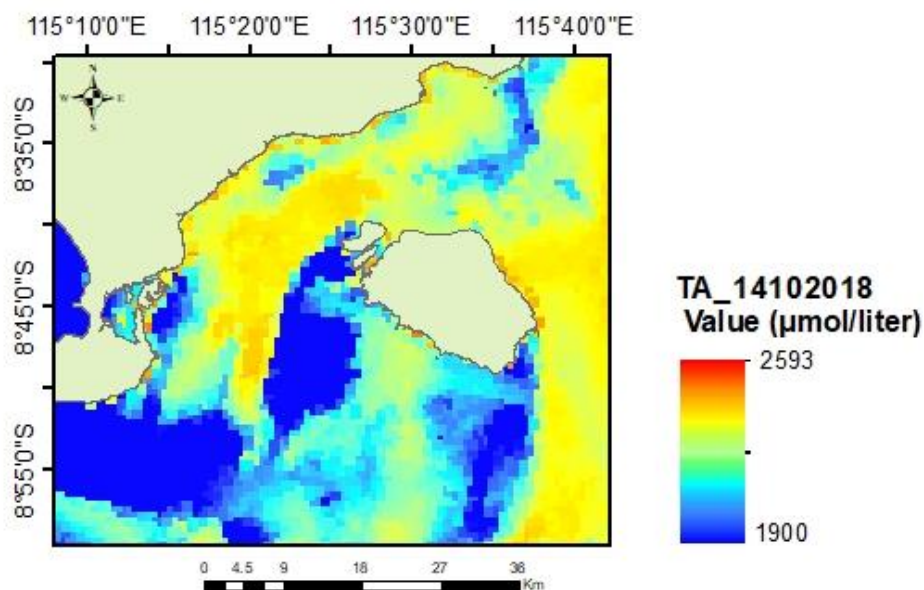


Figure 23. Total alkalinity results from satellite data on 14 October 2018.

Next step is the model validation process. The aim of this process is to know the accuracy of the total alkalinity estimation based on remote sensing. On this local model satellite validation, the total alkalinity estimation which comes from the local model was compared with the ground truth (in-situ data). The total alkalinity dataset that was used in this validation process, were similar to the dataset in the GeoCalVal process from the previous chapter. However, in this satellite validation, the dataset was filtered only at the same passing time of the SMOS (CMEMs) and the Sentinel 3 (SLSTR). The validation result of the total alkalinity estimation analysis can be seen in figure 24. The RMSE result was 65.64 $\mu\text{mol/liter}$, with R^2 value of 0.61. From the figure 24, we also see that the in-situ alkalinity value jumps every 100 $\mu\text{mol/liter}$. This is due to the sensitivity of the total alkalinity test kit, which only able to measure more than 100 $\mu\text{mol/liter}$.

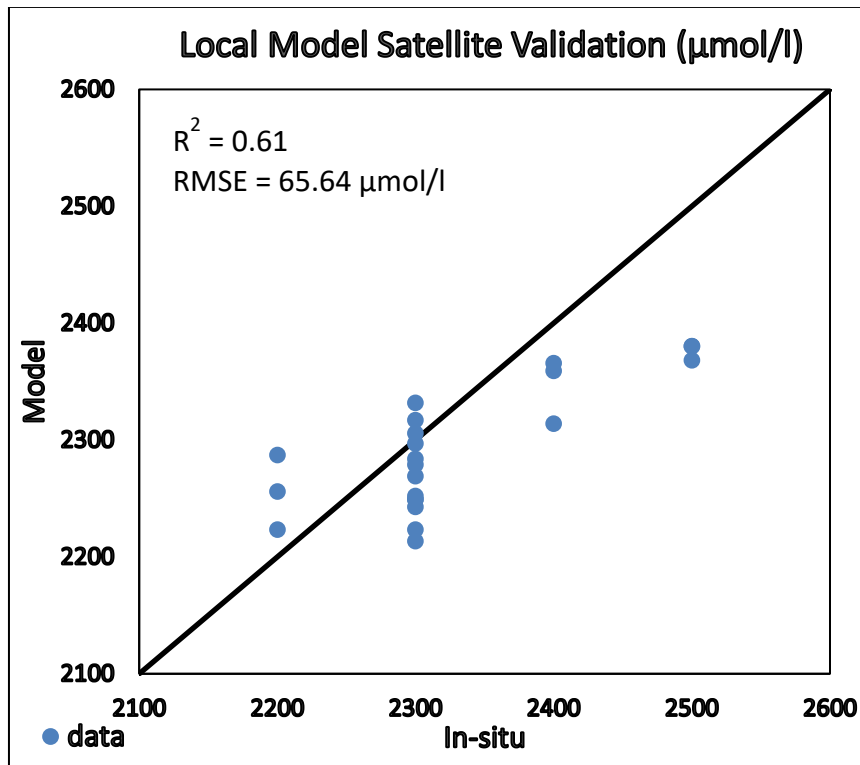


Figure 24. Local model satellite validation.

Further, the local model was used to estimate the total alkalinity variability in the study area for one year. We did this simulation to observe the changes in alkalinity and to evaluate the local model performance in estimating the total alkalinity value in different seasons. The salinity data that were used in estimating monthly total alkalinity value were monthly satellite data from SMOS level 4 (CMEMS). Meanwhile, for the sea surface temperature, we used satellite data of Sentinel 3 (SLSTR) level 1 product which was processed from level 1 to be presented in monthly mean sea surface temperature data. Further, the monthly mean data was calculated using cell statistics by ignoring the no data pixel (NaN).

The total alkalinity estimation was carried out for the period starting from December 2017 to December 2018. The total alkalinity mapping generated from the local model of sea surface total alkalinity can be seen in figure 25 and 26. Figure 25 shows the total alkalinity mapping during the rainy season which started in December 2017 and last until May 2018. It can be seen that the total alkalinity estimation in this period is not reliable, which is indicated by the very low value of the total alkalinity estimation resulted from the local model. Figure 26 shows the total alkalinity mapping during the dry season. In this season, the total alkalinity model gives better estimation than that in the wet season.

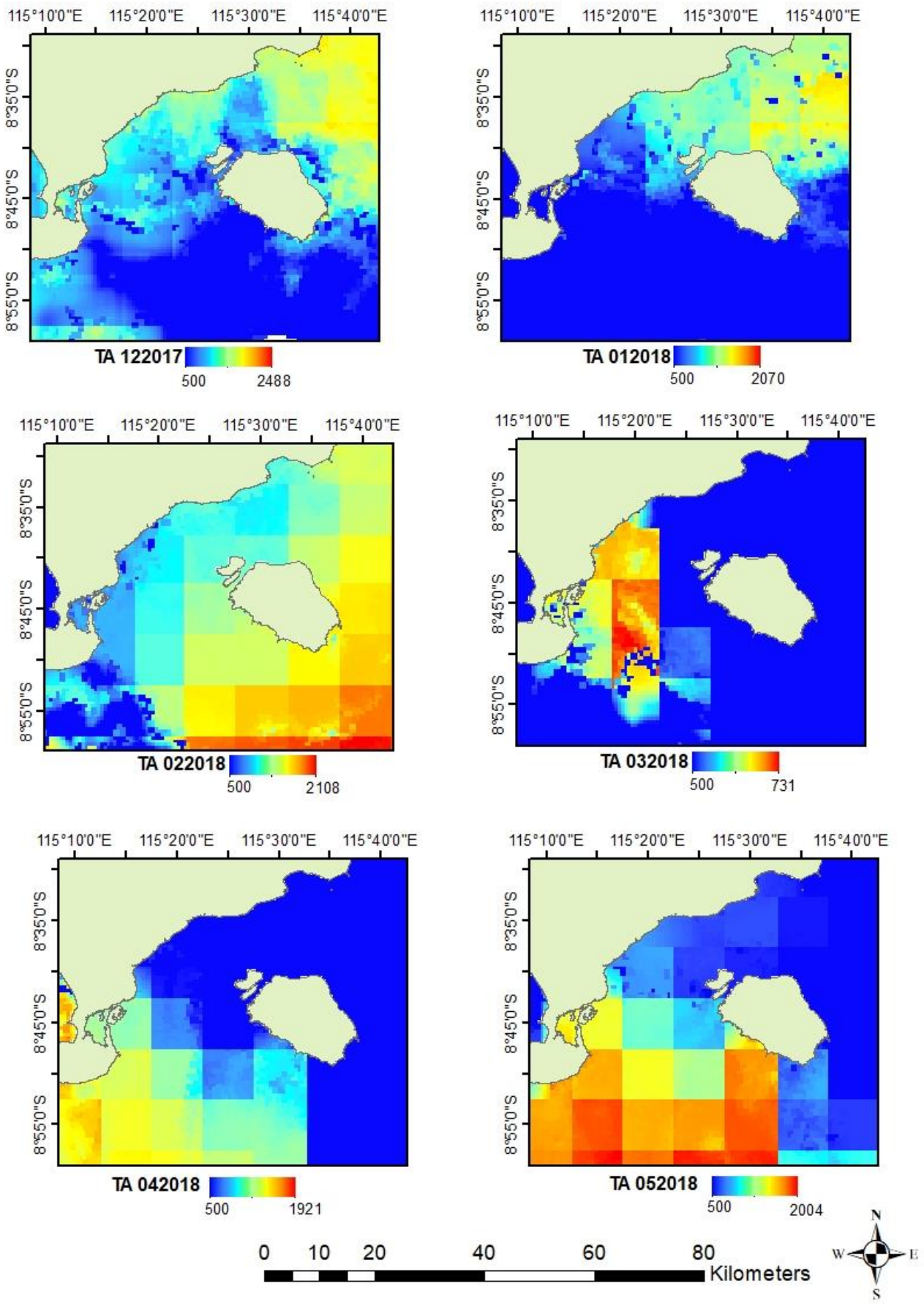


Figure 25. Local model output in wet season on the study area.

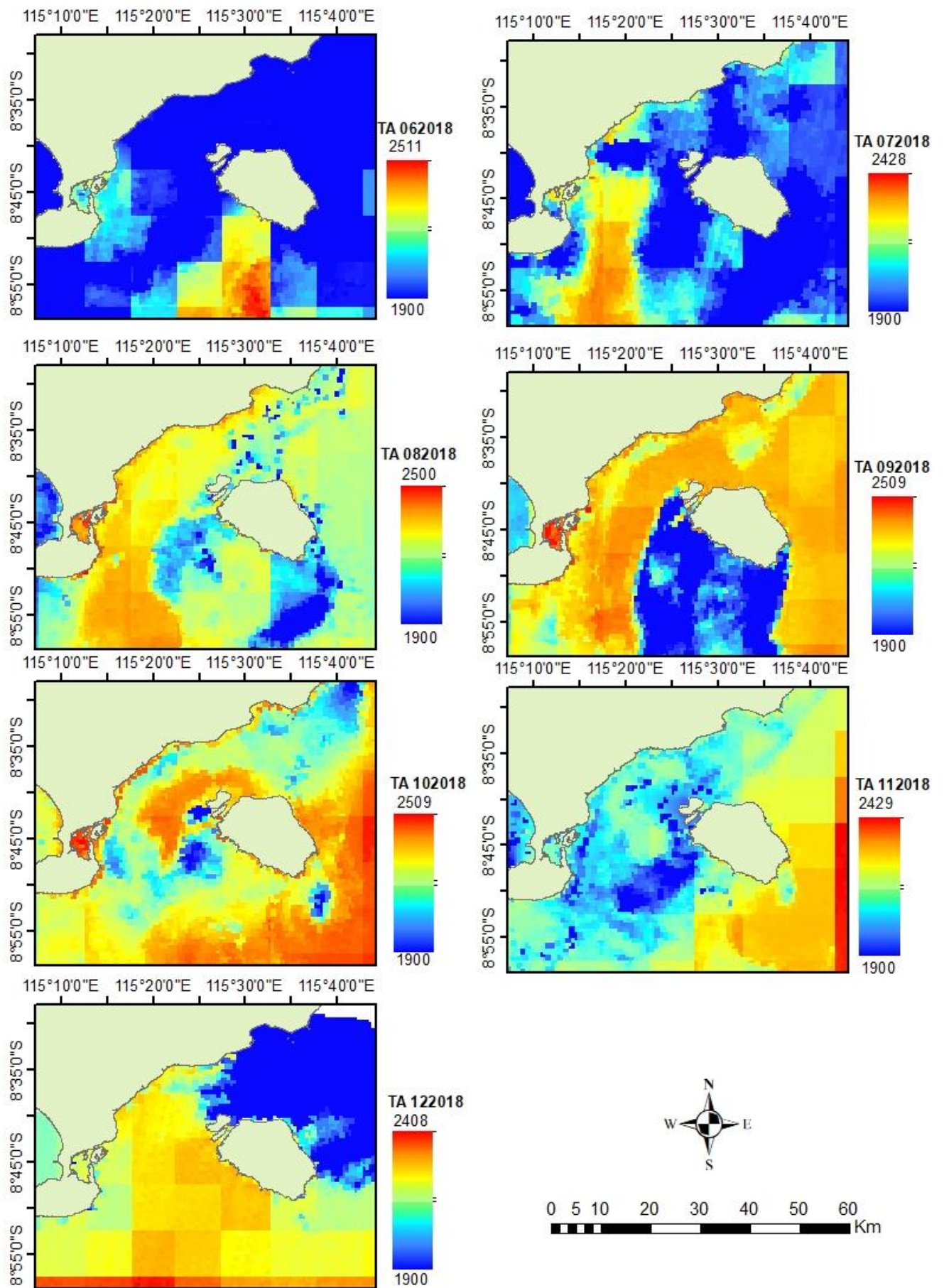


Figure 26. Local model output in dry season on the study area.

Referring to the results of the total alkalinity estimation in the study area above, the total alkalinity tends to be low in the rainy season and high in the dry season. Consequently, Indonesia as a marine country that has various marine organisms such as shells, coral reefs, etc, will be vulnerable to ocean acidification. If the total alkalinity in the ocean is low, these marine organisms will be vulnerable to calcifying in the case of ocean acidification (Schlitzer et al., 2005) since the total alkalinity acts as a buffer against the additional acid in the ocean (Frank J. Millero, Zhang, Lee, & Campbell, 1993).

We extracted further the monthly total alkalinity from the thirteenth total alkalinity maps above to see the interannual variability. The lowest total alkalinity values occurred from December 2017 to May 2018. The values increased from June 2018 and reached the peak in September and October 2018, followed by a decreasing trend in November and December 2018. The local model of sea surface total alkalinity gives a good estimation of the total alkalinity values during the dry season (from June to December 2018) but less reliable when estimating the total alkalinity values during wet season (from December 2017 to May 2018). This is because the fitting model process was using data from September to October, where during this period the salinity values are high (more than 33 PSu). This results in higher accuracy of the total alkalinity on dry season which has high salinity and works less on wet season that has low salinity value (below 33 PSu).

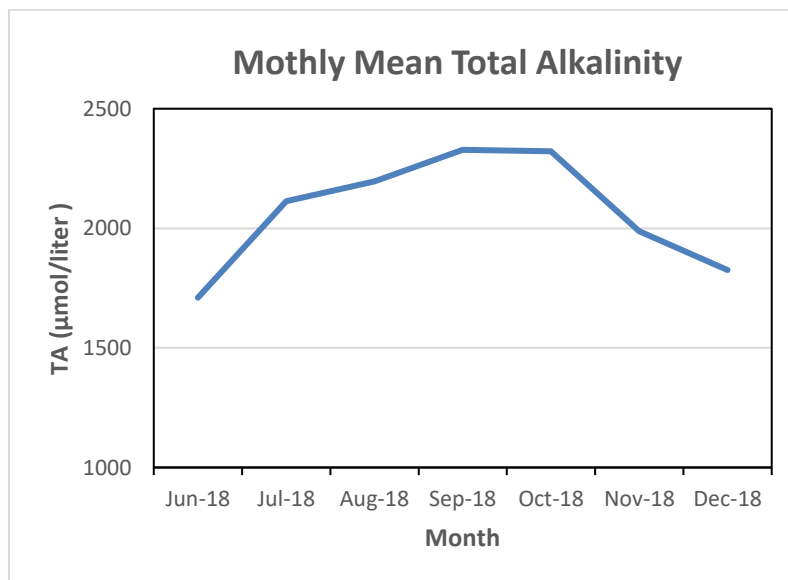


Figure 27. Monthly mean total alkalinity’s estimations from local model output.

Table 10. Monthly total alkalinity’s standard deviation in the study area from local model output.

Month	Dec-17	Jan-18	Feb-18	Mar-18	Apr-18	May-18	Jun-18	Jul-18	Aug-18	Sep-18	Oct-18	Nov-18	Dec-18
T. Alkalinity std. dev (µmol/liter)	241.26	152.92	36.87	79.05	222	52.58	138.82	445.45	196.05	178.01	132.59	297.37	470.28

Table 10 illustrates variability of the monthly total alkalinity in the study area. The highest variability of the monthly total alkalinity is in December 2018, November 2018 and July 2018. These values were affected by the temperature's standard deviation in the study area. The temperature's standard deviation in April, July, November and December 2018 are very high (close to 2), while at the other months are low (close to 1).

4.1.2. Hydrogeochemical Modelling Result

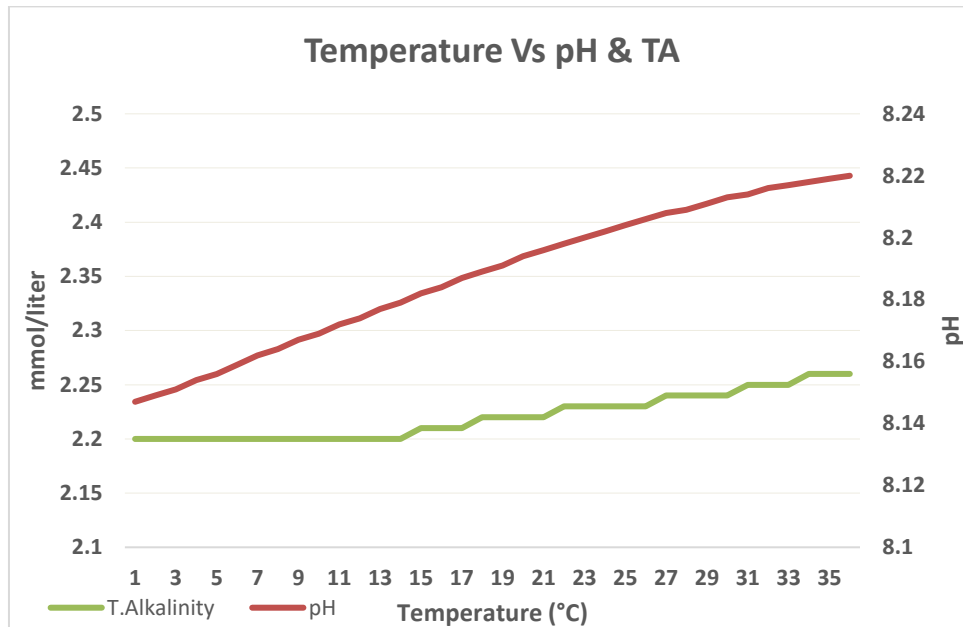


Figure 28. Temperature effect on seawater pH and Total Alkalinity.

In this research, I try to analyse the changes in pH and total alkalinity along with the increase in temperature using a hydro-geochemical model. In this simulation, the composition of seawater and other parameters used are similar with the data in the chapter 3.3. Further, the model was ran from 1 to 35 °C and the TA and pH along the changes in temperature were recorded. Figure 28 depicts the changes in pH and total alkalinity along with the increase in temperature. The total alkalinity concentration which was initially 2.2 mmol/liter at 1 °C, increase slightly to 2.26 mmol/liter at 35°C. Likewise, the pH increased from 8,147 at 1 °C to 8.22 at 35 ° C.

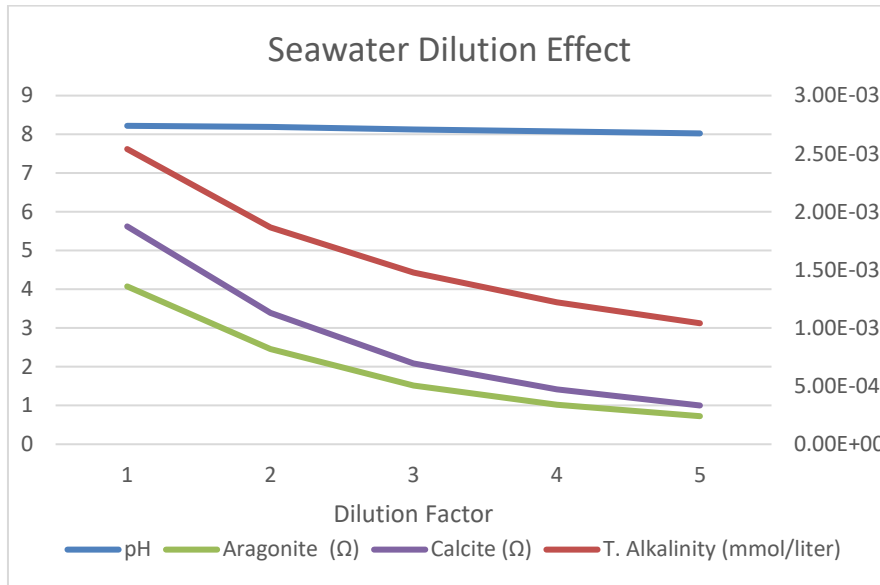


Figure 29. Seawater dilution effect on chemical speciation

Moreover, this study also tries to simulate the effect of salinity changes on pH, aragonite, calcite, and total alkalinity concentration on seawater in the study area, employing the Aqion/Phreeqc software. The simulation was done on 5 steps, each step means 10% dilution of seawater (except step 1, without dilution). Figure 29 depict the changes in pH, aragonite, calcite, and total alkalinity along with the decrease in salinity. The pH value decreases from 8.22 on step 1 (35 PSu) to 8.73 on step 5 (0.0035 PSu). Meanwhile, aragonite, calcite, and total alkalinity drop drastically from step 1 to step 5. Based on the results of the Aqion chemical model, I conclude that the total alkalinity is affected by salinity changes and also affected slightly by temperature changes (see figure 28 and 29). This is comparable with the local model performance of total alkalinity as illustrated in figure 22 of the chapter 3.

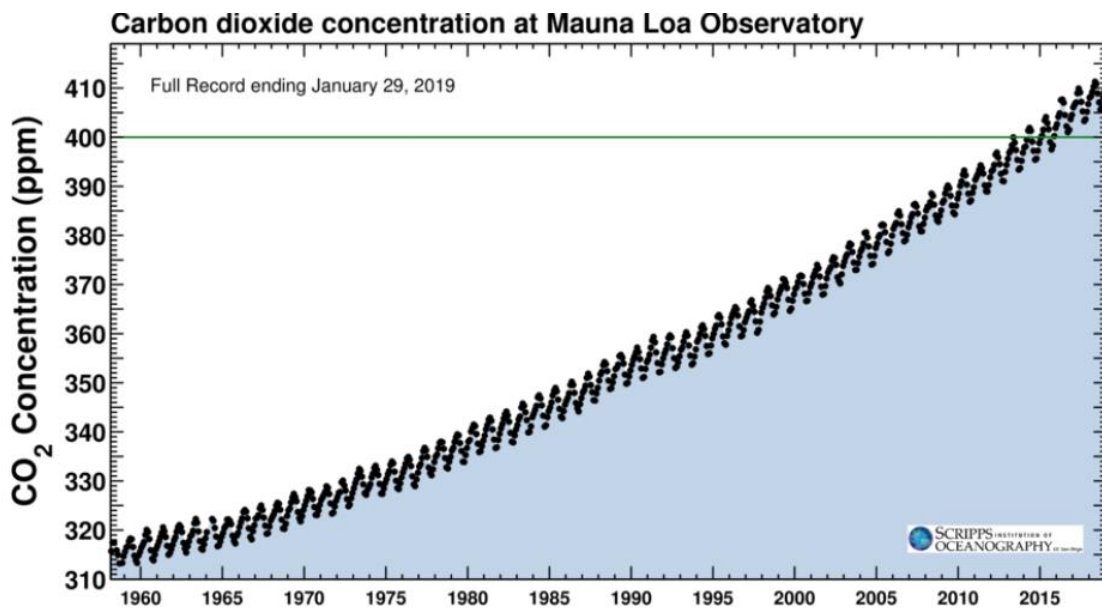


Figure 30. The increase of CO₂ concentration based on Mauna Loa Observatory(Scripps Institution of Oceanography, 2009).

Based on the keelling curve in figure 30, the carbon dioxide concentration in January 2019 is about 411.36 ppm (Scripps Institution of Oceanography, 2009). The atmospheric CO₂ concentration is expected to be higher in the future. The Earth system research laboratory of the NOAA global monitoring division predicts the atmospheric CO₂ concentration increases around 2.3% every 2 years or 1.15% per year (US Department of Commerce, NOAA, 2015). Referring to this projection, I simulate the ocean acidification condition in the study area for the 2 next decades using the Aqion/Phreeqc model.

Figure 31 shows simulation results of the Aqion/Phreeqc chemical model regarding the effects of the projected CO₂ increase on pH, calcite, aragonite, and Dissolve inorganic carbon (DIC) in the study area. The simulation was carried out for two decades from 2019 to 2038. With an increase in the atmospheric CO₂ concentration of 1.15% each year there was a change in chemical speciation of sea water in the study area. Seawater pH in the study area drops from 8.21 to 8.11. Meanwhile, the saturation condition of calcite (Ω) decreases from 5.04 to 4.15. Likewise, aragonite (Ω) decreases from 3.63 to 2.99. However, the effect is different for DIC (Dissolve inorganic carbon), where its concentration increases from 1.98 mmol/liter to 2.03 mmol/liter. As a result, the total concentration of alkalinity remains constant at 2.26 mmol/liter.

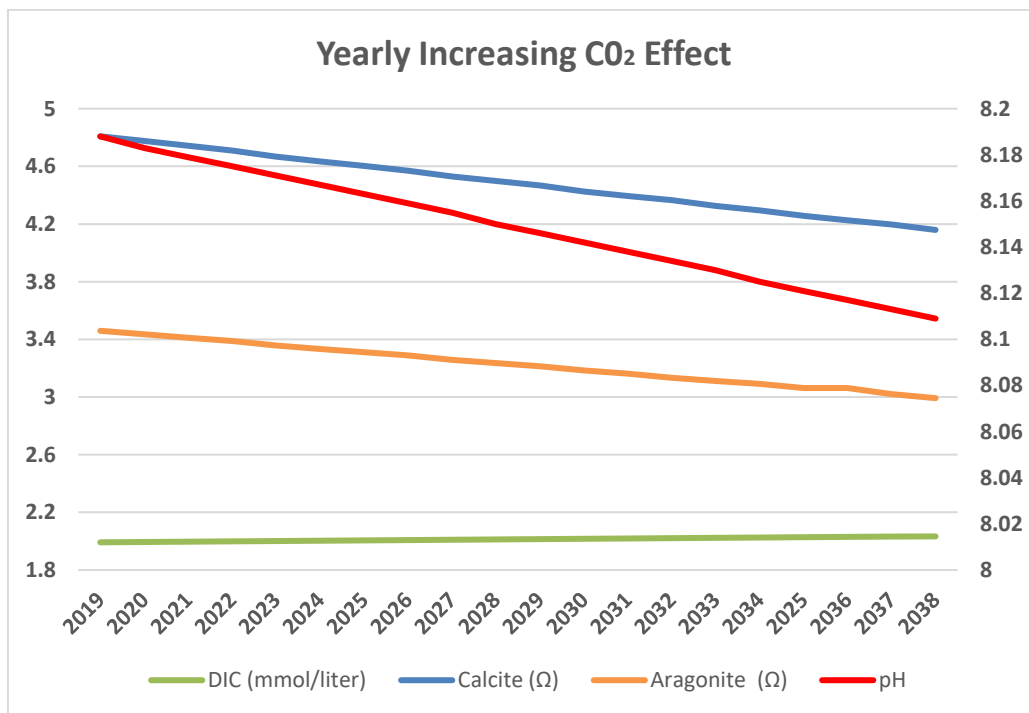


Figure 31. Yearly CO₂ increasing effect on the study area.

Table 11. pH, Calcite, and Aragonite yearly decrease trend.

pH	Calcite (Ω)	Aragonite (Ω)
0.0041	0.0342	0.0244

Table 11 shows the decreasing trend of pH, Calcite and Aragonite saturation based on the Aqion chemical software simulation depicted in Figure 31. With an increase of CO₂ in the study area around 1.15% each year, the calcifying will occur over the next 100 years. Based on calcite saturation indices, calcifying will emerge 118 years later. Calcite saturation will be less than 1 (initially 5.04) with a pH falling to 7.7 (initially 8.21). Furthermore, based on the condition of aragonite saturation indices, calcifying will occur in the study area in the next 107 years. Aragonite saturation state will drop from 3.63 to less than 1 with pH 7.7.

4.2. Discussion

Indonesia is the largest archipelagic country in the world, where most of its territory (60%) is ocean (KKP (Ministry of Maritime Affairs and Fisheries of Indonesia), 2017). Located below the equator, between the Australia and Asia continent, and between the Pacific Ocean and the Indian Ocean, the Indonesian Sea has unique characteristics. Several natural phenomena such as El-Nino La-Nina, Madden-Julian Oscillation, Monsoon, and Indonesian Trough Flow occur at this region and affect the ocean and climate system on a regional or global basis (Li, Gordon, Wei, Gruenberg, & Jiang, 2018). Further, the variability of those natural phenomena is also affected by global warming (Li et al., 2018).

4.2.1. La-Nina El-Nino

El-Nino and La-Nina phenomena, also known as El-Nino Southern Oscillation (ENSO), occur due to extreme temperature fluctuations between the oceans and the atmosphere around the eastern Pacific equator. (N. O. and A. A. US Department of Commerce, 2018). Indonesia's climate was affected by La-Nina and El-Nino, which results in a longer the rainy or dry season in Indonesia (Prasetyo & Nabilah, 2017). Normally, the rainy season on the Java and Bali islands occurs from November to April and the dry season occurs from May to October. However, the period of both seasons can change due to the influence of El-Nino and La-Nina (Krave, Straalen, Verseveld, & Roling, 2007) (Supari et al., 2018). In addition, the phenomenon of El-Nino and La-Nina also affects the duration, intensity and frequency of rain in Indonesia (Supari et al., 2018). Furthermore, the El-Nino phenomenon also has an impact on SST in Indonesia (Napitu, Gordon, & Pujiana, 2015).

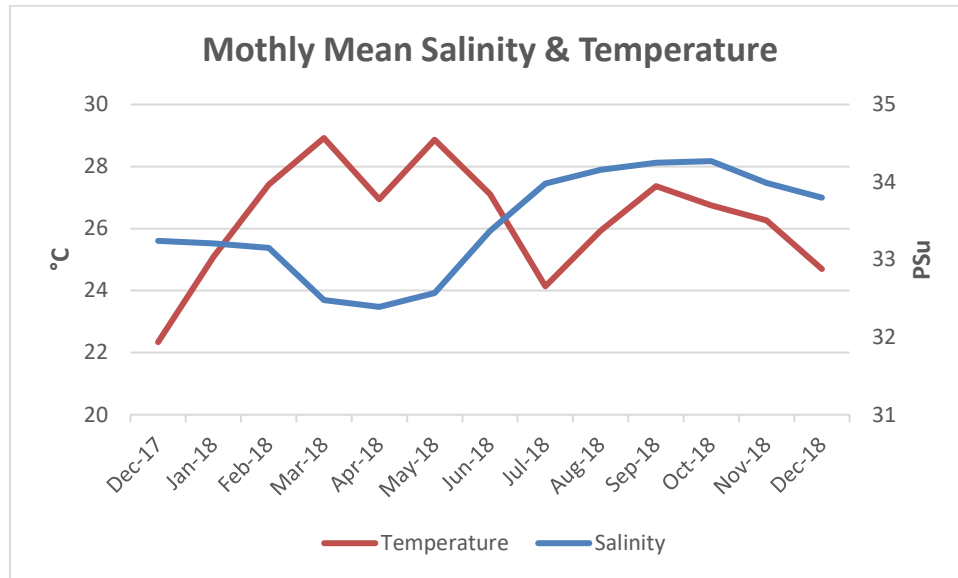


Figure 32. Monthly mean salinity and temperature variability in the study area.

The impact of El-Nino is clearly seen in the study area. If we look at figure 32, the SST from July to November tend to be lower compared to the wet months (February - May), despite the fact that July to November period is a dry season. One characteristic of El-Nino is the low sea surface temperature during the dry season (which is characterized by a little rainfall)(Prasetyo & Nabilah, 2017). Based on the information from BMKG (Meteorological Climatological and Geophysical Agency of Indonesia), during 2018 there has been an increase in the impact of El-Nino since May (Indonesia), 2019). As a result, the rainy season in 2018 which should have started in November, retreated until early January 2019(CNN Indonesia, 2018). Furthermore, the salinity and temperature data in December 2018 is higher than in December 2017, owing to the retreat of the rainy season as a result of the El-Nino phenomenon in the study area.

4.2.2. Monsoon

The Monsoon wind system is a seasonal winds patterns that occurs in Indonesia. This phenomenon occurs because Indonesia lies between the continents of Asia and Australia. Monsoon winds blow from one area to another in a certain direction and period, whereas in other periods the wind blows in the opposite direction. The occurrence of the Monsoon wind is caused by differences in air pressure between Asia and Australia continent. (Nicholls, 1995). Furthermore, this monsoon system also affects the circulation of seawater in Indonesia. The monsoon wind system blows permanently, although the speed is relatively small, so it can create a very good condition for the occurrence of a current pattern. In the North-west monsoon season, the pattern current of Indonesian sea water moves from the South China Sea to the Java Sea (Harvianto & Koropitan, 2015).

There are two Monsoons in Indonesia. The North-West (NW) Monsoon which carries currents and winds from the east, and South-East (SE) Monsoon which carries currents and winds from the west. SE Monsoon usually occurs in June-September where intense heating and low air pressure occurs. Meanwhile, the NW Monsoon season occurs from December to March, which is characterized by high rainfalls (Najid et al., 2012). The SE monsoon is the dry season in Indonesia, where dry and warm air comes from the Australian mainland. whereas in the NW monsoon is the rainy season, where warm and humid air comes from the Eurasian region (Manjunatha, Krishna, & Aswini, 2015).

Sea water density is influenced by temperature and salinity, where this change is affected by the monsoon in the south Asia region (Yuan, Salama, & Su, 2018). Further, the salinity variability is influenced by complex mechanisms such as freshwater flux, horizontal advection, turbulent mixing and diffusion (Yuan et al., 2018). Additionally, seawater mass in Indonesia is affected by the monsoon system, which affects the variability of temperature and salinity of the seawater. The lowest salinity occurred in the 1st Monsoon transition season i.e. from March to April. In the NW monsoon season, which is marked by the rainy season (from November to March), the salinity tends to be low. Meanwhile, the SE monsoon is marked by the dry season (from June to October), where the salinity tends to be high (Najid et al., 2012). This phenomenon is clearly seen in the study area where the lowest salinity occurred in April and the highest in October (see figure 43). The salinity variability of those months is influenced by the presence of Monsoon which causes rain variability in Indonesia (Steinke et al., 2014). This salinity variability is influenced by complex mechanisms such as freshwater flux, horizontal advection, turbulent mixing and diffusion (Yuan et al., 2018)

4.2.3. Madden-Julian Oscillation

Madden-Julian Oscillation (MJO) is an important component of annual variability in the tropic region. This phenomenon affects the climate and weather in the ocean. MJO has a period between 30-100 days/year. The peak occurs during the monsoon summer of Australia, with the strongest MJO occurs in the east of the equator (Zhang, 2005). MJO have an influence on the rain intensity. MJO (Median Julian Oscillation) affects rainfall in Indonesia, with average rainfall anomalies around 5 mm / day on the ocean. Southern parts of Indonesia, such as Java, Bali and Southeast Nusa Tenggara, have been affected by positive rainfall due to MJO. However, the impact of MJO on the ocean (Indian Ocean) is greater than in the maritime area (Hidayat & Kizu, 2010).

MJO together with Monsoon wind affect intra-seasonal variability of SST by 70% (Hidayat & Kizu, 2010). MJO affects the climate of the tropics and equator. Because of MJO, the Indonesian sea tends to be warmer in the rainy season (Dec-Feb) and colder in the dry season (June-Aug). The influence of MJO on SST is high in the wet season and weakens in the dry season, but this weakening also due to the

influence of La-Nina(Napitu et al., 2015). Figure 32 shows that the MJO effect occurs in the study area, where warm temperatures occur in the month of February, and the trend is low from June to August.

4.2.4. Indonesian Through Flow

The Indonesian through flow (ITF) phenomenon is one of the characteristics of the current system in Indonesia. ITF is a marine circulation system in Indonesian waters, where this trajectory of seawater currents carries water masses from the Pacific Ocean to the Indian Ocean. ITF current occurs due to differences in sea level between the Pacific Ocean and the Indian Ocean. the sea surface of the western Pacific Ocean tropic is higher than in the eastern Indian Ocean, because of a pressure gradient (Meyers, Bailey, & Worby, 1995). Indonesian waters, especially on the Makassar Strait, has unique waters characteristic because they are influenced by different seawater masses from the Pacific Ocean and Indian Ocean due to ITF. The ITF transfers the mass of water from the Pacific Ocean to the Indian Ocean through the Indonesian sea area. The mass of seawater carried by the ITF in the Makassar Strait is around 58-80% of the total seawater mass with a depth of 1000 meter (Li et al., 2018).

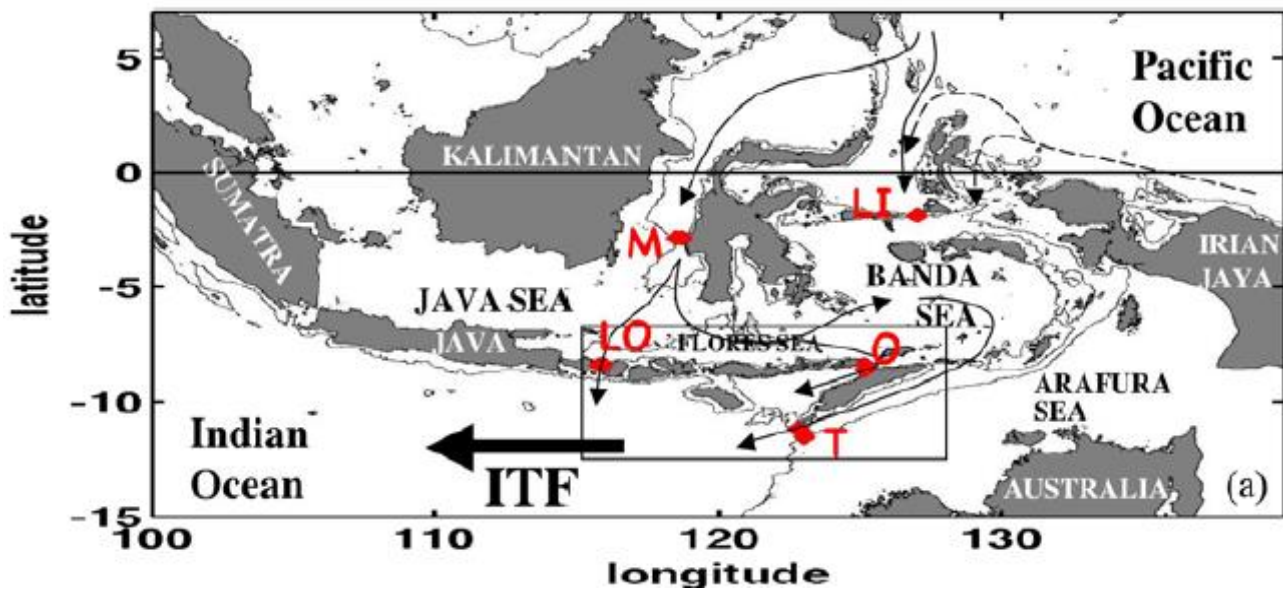


Figure 33. Indonesian Throughflow current.(Sprintall, Wijffels, Molcard, & Jaya, 2009)

Three main exits of ITF are Lombok, Ombai and Timor Straits. ITF is also influenced by the monsoon wind (Sprintall et al., 2009). The maximum ITF flow occurs during the Monsoon SE (second quartile) and weakens at the NW monsoon (fourth quartile) especially on the month of December and January (Manjunatha et al., 2015). The core of ITF flow is between 100-150 m depth (Mayer & Damm, 2012). Apart from being influenced by Monsoon, the reduction in water mass transfer in the ITF is also affected by weakening pacific wind speeds (Li et al., 2018).

Beside affected by local monsoon from Indonesian waters, the ITF interannual variability are also affected by El-Nino phenomenon. The ITF flow is strong during La-Nina and weak during El-Nino. This flow is influenced by the difference in pressure between the Pacific Ocean and the Indian Ocean and is also reinforced by the forcing of currents and wind. This pressure difference is also affected by the variability of temperature and salinity. La-Nina gives refreshment to the Indian ocean and causes variability in salinity. Variability in the 65% transport ITF is influenced by temperature variability. During El-Nino, ITF tends to be low owing to different levels between small Indian and Pacific oceans.

The El-Nino and La-Nina phenomena in the equator area affect the characteristics of the ITF. SST variations occur in the Makassar strait as the main flow of the ITF. In April (transition season) when the wind speeds are low while the solar radiations are high, the weather is warmer. Meanwhile strong winds in June results in SST cooling. Low SST trends occur from December to April. Furthermore, monsoon SE winds increase SST in the Lombok Strait. SST tends to be lower in the dry season (Manjunatha et al., 2015). ITF mass transfer rises during the dry season and falls during the wet season, and decreases during El-Nino (Li et al., 2018). ITF also affects the rainfall patterns in Indonesia (Hu & Sprintall, 2016).

In the Lombok Strait, Indonesian throughflow affects the salinity and temperature of Indonesian seawater (mainly affecting salinity), due to the vertical mixing (Mayer & Damm, 2012). According to Harvianto (2015), the average temperature carried by this flow is around 28.7°C with salinity 33.25 PSu (Harvianto & Koropitan, 2015). If we look at figure 26, this ITF phenomenon clearly occurs in the study area. We can see the shadow of Nusa Penida Island towards the south of the sea area. This indicates that the area has a low temperature and salinity compared to other regions, so that the sea surface alkalinity of the area is also low compared to other areas.

4.2.5. Sea Surface Total Alkalinity Variability

According to the research results that have been obtained in the study area, the variability of the total alkalinity very much depends on the season (wet or dry). This is because the variability of total alkalinity is closely related to the dilution of sea water (Koné & Borges, 2008). The total alkalinity in the study area is also affected by the ITF phenomenon where ITF causes changes in salinity and temperature, which influence the variability of total alkalinity (Fine, Willey, & Millero, 2017). According to a research done by the Indonesian Institute of Science (LIPI), the total alkalinity of Java and surrounding islands is sensitive to the transition of the Monsoon season, and the peak occurs in the Monsoon SE season. In the NW Monsoon season there is a lot of rain, while in the SE Monsoon season it is characterized by little rainfall or drought (Rustam, Bengen, Arifin, & Gaol, 2015). This study reveals that total alkalinity concentrations in the study area were high in the dry season and low in the rainy season.

Spatial and temporal variability of total alkalinity in the surface seawater is largely determined by salinity in the area (Fine et al., 2017). Furthermore, Bakker et.al. (1999) points out that the variability of total alkalinity almost has a linear relationship with the salinity, where the changes are very dependent on rainfall and wind speed in the study area. Beside salinity, the variability of total alkalinity has a correlation with temperature (Bakker, Baar, & Jong, 1999)(Takatani et al., 2014). In the tropics and subtropics region, 80% of the total alkalinity changes depend on the variability of the sea surface salinity (F J Millero, Lee, & Roche, 1998).

Variations in the concentration of alkalinity in the surface layer of sea waters are controlled generally by an increase or reduction in the mass of freshwater that occur through the process of precipitation and evaporation (Triyulianti et al., 2016). TA in areas close to the equator and in shallow seas is relatively high, due to the upwelling process (R. A. Feely et al., 2012) while TA in areas with high latitude is also influenced by sea surface temperature (SST) (Jiang et al., 2014). Further, Jiang (2014) indicates that TA variability in coastal areas is more complex because of the influence from biology activities such as coral reefs. This is because biological activities in warm (tropical) regions, such as CaCO₃ and photosynthetic production, consume nutrients from sea water that affect alkalinity (F J Millero et al., 1998). For instance, NOAA's researchers try to estimate TA using experimental models called 'ocean acidification product suite' (OAPS). They found that the model gives a good estimation for areas that have low Chl-a, but less reliable for areas with high Chl-a (Land et al., 2015)

4.2.6. Future Prediction of Total Alkalinity

The Aqion software (including Phreeqc v.3) was applied to predict the acidification in the study area for the next 20 years. Figure 31 shows, the results of the simulations. The results indicate that the DIC concentration increases slightly. In contrast, the pH, aragonite and calcite saturation decrease. The addition of CO₂ due to the uptake of anthropogenic carbon in the ocean is not directly related to alkalinity (Jiang et al., 2014). The CO₂ increase in seawater will affect the alkalinity in a very long term. It will require several decades, before calcification occurs (Cooley, S., Mathis, J., Yates & and Turley, 2012)

Several studies also found that CO₂ flux from the sea-exchange water has no significant effect on alkalinity changes on the area which has supersaturated of aragonite and calcite condition (Fine et al., 2017) such as in the study area. Furthermore, Feely (2004) found that TA will decrease with the addition of anthropogenic CO₂ after the conditions of aragonite and calcite undersaturated. This condition will occur if pCO₂ reach 1700-2800 μmol/kg which expected to be reached in the next few hundred years (R. a Feely et al., 2004).

The saturation state is high in warm and shallow oceans like in Indonesia. This condition also causes a longer time for total alkalinity to decrease (Koné & Borges, 2008). Therefore, the total alkalinity in the study area will remain constant until the value of aragonite and calcite drops below 1 (under saturated). When this condition is reached, the CO₂ addition will reduce the TA concentration. However, this prediction can be different if there is a drastic change in salinity and temperature since an increase in temperature or salinity can also reduce the CO₂ ability to dissolve in the ocean (Bakker et al., 1999). According to the IPCC 2018 report, the continuous increase of CO₂ concentration in the atmosphere will increase the earth's temperature by 1.5 - 2 degrees globally. Further, this condition will lead to extreme weathers in almost all parts of the world (Masson-Delmotte et al., 2018). In the Indonesian region, heavy rainfalls may occur related to the tropical cyclones. This phenomenon will add more dissolve CO₂ in Indonesia's oceans, because CO₂ flux in the rainy season is 5 times greater than in the dry season (Land et al., 2015). Since the increase of pCO₂ in seawater will cause more carbonate dissolve on seawater, it will ultimately cause a decline in alkalinity conditions in the Indonesian ocean, especially in Nusa Penida (study area).

5. CONCLUSION AND RECOMMENDATION

5.1. Conclusion

The aim of this study is to generate the Total Alkalinity Model to quantify ocean acidification based on sea surface total alkalinity in Badung Strait, Nusa Penida, Bali. The global total sea level alkalinity model was used in this study. This global model was calibrated with the GeoCalVal method using temperature, salinity and total alkalinity data from in situ measurements. From this Calibration and validation results, the local model was produced in accordance with the study area. Then, the local performance of this model was compared with the Aqion chemical model. Finally, this local model was implemented to estimate the amount of sea surface total alkalinity in the study area using remote sensing data. The following is a summary of the findings of this study:

- ❖ Salinity data quality from satellites significantly influences the performance of the sea surface total alkalinity model, because salinity data is an important input parameter to know the sea water geochemistry.
- ❖ Local model sea surface total alkalinity has been successfully run using the SMOS / CMEMS (salinity) and Sentinel 3 (SST) data satellites resulting in a total alkalinity map in the study area with a spatial resolution of 500 m pixels.
- ❖ Since the fitting process was executed during the dry season (high salinity), the local model gives a good estimation of sea surface total alkalinity on high salinity condition (dry season) and less on wet season.
- ❖ We must point out that the Global Ocean Alkalinity model of Lee et al (2005), used here as a starting point, presents a quadratic model structure for both SST (temperature) and PSU (salinity). It is known that quadratic estimation functions work well within a certain range but tend to deviate strongly at lower and higher data input value. So, although we could generate a local model, based on the measurement in September 2018 (dry season), we are concerned and cannot recommend to use this model far beyond the currently observed temperature and salinity data ranges (used for calibration). We recommend to use a longer i.e. a full year observation data set in order to generate a model applicable at full annual time scale.
- ❖ In the Cal-Val process, the resulting RMSE is still large if we compared it with research from Lee. This is because the low precision of the alkalinity test kit due to the titrator was not diluted.
- ❖ In the study area, the monthly variability of sea surface total alkalinity is influenced by the variability of salinity. While on the daily, sea surface total alkalinity model is influenced by the variability of SST. This can be seen from the large monthly standard deviation of the total alkalinity model which occurs when the SST monthly standard deviation is also large.

- ❖ The local model total alkalinity, remote sensing-based, has the same performance as the Aqion (Phreeqc) chemical model. Both models are very sensitive in salinity changes and slightly sensitive in temperature changes.
- ❖ The weather and global phenomena such as Monsoon wind, La-Nina and El-Nino, Madden-Julian Oscillation, and Indonesia Through Flow, affect the sea surface total alkalinity condition on the study area.
- ❖ Also, the El-Nino seems to effect on the total alkalinity in the study area. The phenomenon can be seen with higher sea surface total alkalinity in December 2018 compared to December 2017
- ❖ Monsoon winds have an impact on the seasonal variability of the total alkalinity in the study area. High total alkalinity occurs in SE monsoon and low total alkalinity at NW monsoon.
- ❖ Madden-Julian had an impact on SST in the study area. However, this phenomenon does not have a significant effect on the monthly Total Alkalinity variability.
- ❖ The Indonesian Through Flow phenomenon appears in the study area from June to November 2018. It was characterized by low temperatures and high salinity of seawater in the south of Nusa Penida
- ❖ To determine the changes in total alkalinity due to ocean acidification, it would take longer time because the study areas are located on the equator that have high aragonite and calcite saturation state.
- ❖ Global warming which causes climate change could accelerate the effect of ocean acidification on total alkalinity in the study area.

5.2. Recommendation

- ❖ For further research, when using the practical field total alkalinity titrator kit (i.e. no chemical laboratory available), we recommend to use a small dilution series for the titrator measurement with the total alkalinity test kit, when doing the in-situ alkalinity measurement. This additional procedure will increase total alkalinity field measurement accuracy and give better model fittings with smaller RMSE.
- ❖ We recommend to extend the combined sea surface temperature (SST), sea surface salinity (SSS), total alkalinity (and accompanying seawater chemistry) measurements over a longer e.g. annual period for example using automated CTD (conductivity-temperature-pressure) loggers and regular (e.g. weekly total alkalinity sampling and measurements). So, model fitting process in the wet season (expected low salinity, and different temperature) can then be done, to produce a local model that can estimate the total alkalinity in all seasons.

- ❖ The combination of the remote sensing data and model with the chemical model (Aqion/Phreeqc) can give better modeling result on Sea Surface Total Alkalinity estimation, especially the monitoring of the spatial and temporal trends in the regional and coastal areas.
- ❖ The geochemical model (Aqion v.6.7.3, an interface based on Phreeqc v3+), can be used to calculate seawater speciations (i.e. chemical element concentrations) the total alkalinity concentration on low salinity, then apply it on local model in wet season. It can also be used to estimate the effects of other constituents (carbon dioxide, sulphur, borate, nitrogen, phosphate species) and also biological processes (e.g. photosynthesis) on ocean acidification. This modelling however requires good understanding of chemical phase equilibria and also non equilibrium processes.
- ❖ Further research is needed to figure out the effect of biological activity on the performance of this local model total alkalinity. This is because the study area was located on a coral reef area which has a lot of biological activities.
- ❖ To study the effect of ocean acidification on the total alkalinity, it is also very useful to add the aragonite and calcite mineral saturation state changes on the research. These are the current mostly used acidification “parameters” in marine and climate change research. These chemical indices also directly affect coral reef health, growth, and functioning.

LIST OF REFERENCES

- Allard, D.; Baret, F.; Weiss, M. (2006). Influence of landscape spatial heterogeneity on the non-linear estimation of leaf area index from moderate spatial resolution remote sensing data. *Remote Sensing of Environment*, 105(4), 286–298. <https://doi.org/10.1016/j.rse.2006.07.013>
- Aqion. (2012). Validation of Water Sample Data. Retrieved January 8, 2019, from <http://www.aqion.de/site/78>
- Bakker, D. C. E., Baar, H. J. W. De, & Jong, E. De. (1999). The dependence on temperature and salinity of dissolved inorganic carbon in East Atlantic surface waters.
- BMKG. (2018). Prakiraan Cuaca Indonesia | BMKG. Retrieved January 11, 2019, from <http://www.bmkg.go.id/cuaca/prakiraan-cuaca-indonesia.bmkg>
- CNN Indonesia. (2018). BMKG Prediksi El Nino Terjadi Akhir September hingga Oktober. Retrieved February 14, 2019, from <https://www.cnnindonesia.com/nasional/20180911174013-20-329429/bmkg-prediksi-el-nino-terjadi-akhir-september-hingga-oktober>
- Cooley, S., Mathis, J., Yates, K., & and Turley, C. eds. (2012). *Ocean Acidification, FAQ*. <https://doi.org/10.17226/12904>
- Copernicus. (2012). Global Observed Ocean Physics Temperature Salinity Heights MLD Geostrophic Currents Sea Surface Salinity and Sea Surface Density Reprocessing-CMEMS. Retrieved February 18, 2019, from http://marine.copernicus.eu/services-portfolio/access-to-products/?option=com_csw&view=details&product_id=MULTIOBS_GLO_PHY_REP_015_002
- Doney, S. C., Fabry, V. J., Feely, R. A., & Kleypas, J. A. (2009). Ocean Acidification: The Other CO₂ Problem. *Annual Review of Marine Science*, 1(1), 169–192. <https://doi.org/10.1146/annurev.marine.010908.163834>
- Dore, J. E., Lukas, R., Sadler, D. W., Church, M. J., & Karl, D. M. (2009). Physical and biogeochemical modulation of ocean acidification in the central North Pacific. *Proceedings of the National Academy of Sciences*, 106(30), 12235–12240. <https://doi.org/10.1073/pnas.0906044106>
- Eakin, C. M., Nim, C. J., Brainard, R. E., Christoph, A., Elvidge, C., Gledhill, D., ... Mumby, P. J. (2010). Monitoring Coral Reefs from Space. *Oceanography*, 23(4), 119–133. <https://doi.org/10.5670/oceanog.2011.65>
- Eisler, R. (2012). *Oceanic Acidification*. Boca Raton, Florida: CRC Press.
- ESA. (2018a). Missions - Sentinel Online.
- ESA. (2018b). Sentinel-3 - Data Products - Synergy - Sentinel Online.
- ESA. (2018c). SMOS on Acid.
- Feely, R. A., Sabine, C. L., Byrne, R. H., Millero, F. J., Dickson, A. G., Wanninkhof, R., ... Greeley, D. (2012). Decadal changes in the aragonite and calcite saturation state of the Pacific Ocean. *Global Biogeochemical Cycles*, 26(3), 1–15. <https://doi.org/10.1029/2011GB004157>
- Feely, R. a, Sabine, C. L., Lee, K., Berelson, W., Kleypas, J., Fabry, V. J., & Millero, F. J. (2004). Impact of Anthropogenic CO₂ on the CaCO₃ System in the Oceans Author(s): Richard A. Feely, Christopher L. Sabine, Kitack Lee, Will Berelson, Joanie Kleypas, Victoria J. Fabry and Frank J. Millero Source:, 305(5682), 362–366.
- Fine, R. A., Willey, D. A., & Millero, F. J. (2017). Global variability and changes in ocean total alkalinity from Aquarius satellite data. *Geophysical Research Letters*, 44(1), 261–267. <https://doi.org/10.1002/2016GL071712>
- GEOMAR Helmholtz Centre for Ocean Research Kiel. (2015). BIOACID – Biological Impacts of Ocean Acidification – BIOACID: Biological Impacts of Ocean Acidification. Retrieved February 21, 2019, from <https://www.oceanacidification.de/bioacid-biological-impacts-of-ocean-acidification/?lang=en>
- Gledhill, D., Wanninkhof, R., & Eakin, C. M. (2009). Observing Ocean Acidification from Space. *Oceanography*, 22(4), 48–59.
- Harvianto, L., & Koropitan, A. F. (2015). Analisis Diagram T-S Berdasarkan Parameter Oseanografis di Perairan Selat Lombok, (October).
- Hedley, J. D., Roelfsema, C., Brando, V., Giardino, C., Kutser, T., Phinn, S., ... Koetz, B. (2018). Remote Sensing of Environment Coral reef applications of Sentinel-2 : Coverage , characteristics , bathymetry and benthic mapping with comparison to Landsat 8. *Remote Sensing of Environment*, 216(July), 598–614. <https://doi.org/10.1016/j.rse.2018.07.014>
- Hidayat, R., & Kizu, S. (2010). Influence of the Madden-Julian Oscillation on Indonesian rainfall variability in austral summer. *International Journal of Climatology*, 30(12), 1816–1825. <https://doi.org/10.1002/joc.2005>
- Hu, S., & Sprintall, J. (2016). Interannual variability of the Indonesian Throughflow: The salinity effect. *Journal of Geophysical Research: Oceans*, 121, 2596–2615. <https://doi.org/10.1002/2015JC011495>.Received

- Indonesia), B. C. and G. A. of. (2019). Index El-Nino di Indonesia. Retrieved February 14, 2019, from <https://www.bmkg.go.id/iklim/informasi-index-elnino.bmkg>
- IPCC. (2007). Climate Change 2007: Working Group I: The Physical Science Basis.
- Jennerjahn, T. C. (2012). Earth-Science Reviews Biogeochemical response of tropical coastal systems to present and past environmental change. *Earth Science Reviews*, 114(1–2), 19–41. <https://doi.org/10.1016/j.earscirev.2012.04.005>
- Jiang, Z., Tyrrell, T., Hydes, D. J., Dai, M., Hartman, S. E., Tyrrell, T., ... Hartman, S. E. (2014). Global Biogeochemical Cycles, 729–742. <https://doi.org/10.1002/2013GB004678>. Received
- KKP (Ministry of Maritime Affairs and Fisheries of Indonesia). (2017). Maritim Indonesia, Kemewahan Yang Luar Biasa. Retrieved February 14, 2019, from <https://kkp.go.id/artikel/2233-maritim-indonesia-kemewahan-yang-luar-biasa>
- Knudby, A., Pittman, S. J., Maina, J., & Rowlands, G. (2014). Remote Sensing and Modeling, 5, 103–134. <https://doi.org/10.1007/978-3-319-06326-3>
- Koné, Y. J. M., & Borges, A. V. (2008). Dissolved inorganic carbon dynamics in the waters surrounding forested mangroves of the Ca Mau Province (Vietnam). *Estuarine, Coastal and Shelf Science*, 77(3), 409–421. <https://doi.org/10.1016/j.ecss.2007.10.001>
- Krave, A. S., Straalen, N. M. van, Verseveld, H. W. van, & Roling, W. F. M. (2007). Influence of the El Niño and La Niña climate events and litter removal on inorganic nitrogen dynamics in pine forest soils on Central Java, Indonesia. *European Journal of Soil Biology*, 43(5), 39–47. <https://doi.org/10.1016/j.ejsobi.2006.03.005>
- Land, P. E., Shutler, J. D., Findlay, H. S., Girard-Ardhuin, F., Sabia, R., Reul, N., ... Bhadury, P. (2015). Salinity from space unlocks satellite-based assessment of ocean acidification. *Environmental Science and Technology*, 49(4), 1987–1994. <https://doi.org/10.1021/es504849s>
- Lee, K., Tong, L. T., Millero, F. J., Sabine, C. L., Dickson, A. G., Goyet, C., ... Key, R. M. (2006). Global relationships of total alkalinity with salinity and temperature in surface waters of the world's oceans. *Geophysical Research Letters*, 33(19), 1–5. <https://doi.org/10.1029/2006GL027207>
- Li, M., Gordon, A. L., Wei, J., Gruenburg, L. K., & Jiang, G. (2018). Multi-decadal timeseries of the Indonesian throughflow. *Dynamics of Atmospheres and Oceans*, 81(February), 84–95. <https://doi.org/10.1016/j.dynatmoce.2018.02.001>
- Manjunatha, B. R., Krishna, K. M., & Aswini, A. (2015). Anomalies of the Sea Surface Temperature in the Indonesian Throughflow Regions : A Need for Further Investigation, 2–8.
- Masson-Delmotte, V., Zhai, P., Pörtner, H.-O., Roberts, D., Skea, J., Shukla, P. R., ... Waterfield, T. (2018). *IPCC Special Report 1.5 - Summary for Policymakers*. *Ipc*. <https://doi.org/10.1017/CBO9781107415324>
- Mayer, B., & Damm, P. E. (2012). The Makassar Strait throughflow and its jet, 117(July), 1–14. <https://doi.org/10.1029/2011JC007809>
- Meyers, G., Bailey, R. J., & Worby, A. P. (1995). Geostrophic transport of Indonesian throughflow. *Deep-Sea Research Part I*, 42(7), 1163–1174. [https://doi.org/10.1016/0967-0637\(95\)00037-7](https://doi.org/10.1016/0967-0637(95)00037-7)
- Millero, F. J. (1995). Thermodynamics of the carbon dioxide system in the oceans. *Science*, 59(4), 661–677.
- Millero, F. J., Lee, K., & Roche, M. P. (1998). The distribution of total alkalinity in the surface waters. *Marine Chemistry*, 60, 111–130.
- Millero, F. J., & Leung, W. H. (1978). Errata. The thermodynamics of seawater at one atmosphere. *American Journal of Science*, 278(November 1976), 1024. <https://doi.org/10.2475/ajs.276.9.1035>
- Millero, F. J., Zhang, J. Z., Lee, K., & Campbell, D. M. (1993). Titration alkalinity of seawater. *Marine Chemistry*, 44(2–4), 153–165. [https://doi.org/10.1016/0304-4203\(93\)90200-8](https://doi.org/10.1016/0304-4203(93)90200-8)
- Najid, A., Pariwono, J. I., Bengen, D. G., Nurhakim, S., & Atmadipoera, A. S. (2012). Pola Musiman dan Antar Tahunan Salinitas Permukaan Laut Di Perairan Utara Jawa-Madura. *Maspri Journal*, 4(2), 168–177.
- Napitu, A. M., Gordon, A. L., & Pujiana, K. (2015). Intraseasonal sea surface temperature variability across the Indonesian seas. *Journal of Climate*, 28(22), 8710–8727. <https://doi.org/10.1175/JCLI-D-14-00758.1>
- Nardelli, B. B. (2012). A Novel Approach for the High-Resolution Interpolation of In Situ Sea Surface Salinity. *Journal of Atmospheric and Oceanic Technology*, 29(6), 867–879. <https://doi.org/10.1175/JTECH-D-11-00099.1>
- Nicholls, N. (1995). All-India Summer Monsoon Rainfall and Sea Surface Temperatures around Northern Australia and Indonesia. *American Meteorological Society*, 5.
- NOAA. (2014). NOAA Coral Reef Watch Ocean Acidification Products.
- NOAA. (2017a). Ocean Acidification: Saturation State Dataset | Science On a Sphere.
- NOAA. (2017b). Ocean Acidification: Surface pH Dataset | Science On a Sphere.

- Prasetyo, Y., & Nabilah, F. (2017). Pattern Analysis of El Nino and la Nina Phenomenon Based on Sea Surface Temperature (SST) and Rainfall Intensity using Oceanic Nino Index (ONI) in West Java Area. *IOP Conference Series: Earth and Environmental Science*, 98(1). <https://doi.org/10.1088/1755-1315/98/1/012041>
- Putri, M. (2015). Variation of ocean pH in the Indonesia waters, (October). <https://doi.org/10.1063/1.4930701>
- Ritter, M. E. (2016). Digging Deeper: Ocean Acidification. Retrieved January 9, 2019, from http://www.earthonlinemedia.com/ebooks/tpe_3e/earth_system/digging_deeper_ocean_acidification.html
- Rustam, A., Bengen, D. G., Arifin, Z., & Gaol, J. L. (2015). Dinamika Dissolved Inorganic Carbon (Dic) Di Ekosistem Lamun Pulau Pari. *Jurnal Segara*, 10(1). <https://doi.org/10.15578/segara.v10i1.13>
- Safitri, M., & Putri, M. (2009). Kondisi Keasaman (pH) Laut Indonesia, 73–87.
- Salama, M. S., Velde, R. Van Der, Woerd, H. J. Van Der, Kromkamp, J. C., Philippart, C. J. M., & Joseph, A. T. (2012). Technical Note : Calibration and validation of geophysical observation models, 2195–2201. <https://doi.org/10.5194/bg-9-2195-2012>
- Schlitzer, R., Lindsay, K., Mouchet, A., Key, R. M., Bopp, L., Najjar, R. G., ... Plattner, G.-K. (2005). Anthropogenic ocean acidification over the twenty-first century and its impact on calcifying organisms. *Nature*, 437(7059), 681–686. <https://doi.org/10.1038/nature04095>
- Scripps Institution of Oceanography, U. S. D. (2009). The Keeling Curve | A daily record of atmospheric carbon dioxide from Scripps Institution of Oceanography at UC San Diego. Retrieved January 31, 2019, from <https://scripps.ucsd.edu/programs/keelingcurve/>
- Sprintall, J., Wijffels, S. E., Molcard, R., & Jaya, I. (2009). Direct estimates of the Indonesian Throughflow entering the Indian Ocean : 2004 – 2006, 114(July), 2004–2006. <https://doi.org/10.1029/2008JC005257>
- Steinke, S., Mohtadi, M., Prange, M., Varma, V., Pittauerova, D., & Fischer, H. W. (2014). Mid- to Late-Holocene Australian-Indonesian summer monsoon variability. *Quaternary Science Reviews*, 93, 142–154. <https://doi.org/10.1016/j.quascirev.2014.04.006>
- Supari, Tangang, F., Salimun, E., Aldrian, E., Sopaheluwakan, A., & Juneng, L. (2018). ENSO modulation of seasonal rainfall and extremes in Indonesia. *Climate Dynamics*, 51(7–8), 2559–2580. <https://doi.org/10.1007/s00382-017-4028-8>
- Takahashi, T., Sutherland, S. C., Chipman, D. W., Goddard, J. G., & Ho, C. (2014). Climatological distributions of pH, pCO₂, total CO₂, alkalinity, and CaCO₃ saturation in the global surface ocean. *Marine Chemistry*, 164, 95–125. <https://doi.org/10.1016/j.marchem.2014.06.004>
- Takatani, Y., Enyo, K., Iida, Y., Kojima, A., Nakano, T., Sasano, D., ... Ishii, M. (2014). Relationships between total alkalinity in surface water and sea surface dynamic height in the Pacific Ocean. *Journal of Geophysical Research: Oceans*, 119, 2806–2814. <https://doi.org/10.1002/2013JC009739>. Received
- Triyulianti, I., Widagti, N., Rintika, W. E., & Tenggono, M. (2012). Distribusi Vertikal Ph Dan Alkalinitas Perairan Selatan Jawa Dan Samudera Hindia. In *Natioanal Colloquium for Marine and Fisheries* (p. 7).
- Triyulianti, I., Yunanto, A., Pradisty, N. A., Islamy, F., Putri, M. R., & Oseanografi, D. (2016). Sistem karbon laut di perairan laut maluku dan laut sulawesi, 2018.
- United Nations. (2015). Oceans - United Nations Sustainable Development. Retrieved January 31, 2019, from <https://www.un.org/sustainabledevelopment/oceans/>
- US Department of Commerce, NOAA, E. S. R. L. (2015). ESRL Global Monitoring Division - Global Greenhouse Gas Reference Network. Retrieved from <https://www.esrl.noaa.gov/gmd/ccgg/trends/ff.html>
- US Department of Commerce, N. N. C. for E. I. (2017). World Ocean Atlas 2013 version 2.
- US Department of Commerce, N. O. and A. A. (2018). What are El Nino and La Nina? Retrieved February 14, 2019, from <https://oceanservice.noaa.gov/facts/ninonina.html>
- Yang, D. T., Liu, S. M., & Shan, X. J. (2013). Detection of coral distribution change in recent decades with satellite remote sensing. *Proceedings of the 2013 6th International Congress on Image and Signal Processing, CISP 2013*, 2(Cisp), 830–834. <https://doi.org/10.1109/CISP.2013.6745280>
- Yuan, X., Salama, M. S., & Su, Z. (2018). Observational Perspective of Sea Surface Salinity in the Southwestern Indian Ocean and Its Role in the South Asia Summer Monsoon. *MDPI Journal Remote Sensing*, 1930, 10. <https://doi.org/10.3390/rs10121930>
- Zhang, C. (2005). Madden-Julian Oscillation. *Rev. Geophys*, 43, RG2003. <https://doi.org/10.1029/2004RG000158.1>

APPENDICES

APPENDIX 1: Sampling point coordinate on fieldwork measurement.

		Point									
		1	2	3	4	5	6	7	8	9	10
D1_T6	Lat	-8.69264	-8.68602	-8.6812	-8.67444	-8.66978	-8.66191	-8.65527	-8.6494	-8.64316	-8.63822
	Long	115.4258	115.4199	115.4129	115.4048	115.3984	115.3916	115.3854	115.3791	115.3734	115.367
D2_T1	Lat	-8.68371	-8.67641	-8.67184	-8.66773	-8.66346	-8.65923	-8.65536	-8.6522	-8.64848	-8.64527
	Long	115.4758	115.4808	115.4896	115.4981	115.5068	115.5154	115.5235	115.5305	115.5382	115.5464
D3_T2	Lat	-8.68358	-8.67725	-8.66599	-8.65717	-8.648	-8.63901	-8.62973	-8.62065	-8.61119	-8.60219
	Long	115.474	115.48	115.479	115.4766	115.4759	115.4739	115.473	115.4709	115.4702	115.4684
D4_T3	Lat	-8.68398	-8.67449	-8.66921	-8.66322	-8.65808	-8.64817	-8.64385	-8.63821	-8.63223	-8.62528
	Long	115.4754	115.4803	115.4753	115.4687	115.4607	115.4534	115.4467	115.4411	115.4323	115.4259
D5_T3	Lat	-8.68575	-8.67446	-8.66994	-8.66289	-8.65647	-8.65033	-8.6439	-8.638	-8.63267	-8.62607
	Long	115.4731	115.4798	115.4749	115.4671	115.4597	115.4533	115.4456	115.4405	115.4314	115.4246
D6_T2	Lat	-8.6869	-8.67563	-8.66603	-8.65734	-8.64881	-8.63955	-8.62979	-8.62048	-8.61138	-8.60215
	Long	115.4742	115.4794	115.4785	115.4766	115.4743	115.4738	115.4726	115.4713	115.469	115.4682
D7_T5	Lat	-8.69342	-8.68728	-8.67979	-8.67356	-8.66674	-8.66115	-8.65435	-8.64794	-8.64177	-8.63637
	Long	115.4267	115.4198	115.4325	115.4256	115.4192	115.4126	115.4052	115.3982	115.3921	115.3856
D8_T4	Lat	-8.69314	-8.68689	-8.66788	-8.6587	-8.65265	-8.64634	-8.63941	-8.63303	-8.62687	-8.62258
	Long	115.4266	115.4199	115.4423	115.4391	115.4326	115.426	115.4187	115.412	115.4054	115.3999
D9_T4	Lat	-8.6932	-8.68701	-8.66808	-8.65886	-8.65279	-8.64638	-8.63957	-8.63313	-8.62698	-8.62265
	Long	115.4264	115.4198	115.4422	115.4392	115.4325	115.4258	115.4187	115.4121	115.4057	115.4
D10_T5	Lat	-8.6932	-8.6868	-8.67992	-8.67364	-8.66751	-8.66123	-8.65442	-8.648	-8.64202	-8.63643
	Long	115.4264	115.4201	115.4323	115.4258	115.4193	115.4127	115.4053	115.3986	115.3922	115.3857
D11_T6	Lat	-8.69312	-8.68709	-8.68086	-8.67455	-8.66804	-8.66149	-8.65483	-8.64902	-8.64293	-8.63813
	Long	115.4265	115.4199	115.4134	115.4069	115.4002	115.3929	115.3863	115.3796	115.3737	115.3671
D12_T1	Lat	-8.68485	-8.67696	-8.67277	-8.6681	-8.66368	-8.65923	-8.65554	-8.65182	-8.6487	-8.64548
	Long	115.4749	115.4813	115.489	115.4982	115.5067	115.5156	115.5233	115.5302	115.5383	115.5464

Note: Lat : Latitude.
 Long : Longitude.
 D1_T6 : Day 1 measurement on Trajectory number 6.

APPENDIX 2: Schedule of satellite pass on the study area.

Date	Satellite			In-Situ Measurement			
	Type	SZA	Time pass	SZA start	start time	SZA end	end time
10-Sep-18	Sentinel-3B	38.03037	9:53	58.61483	7:50	24.2307	13:00
	Sentinel-3A	37.91746	9:54				
	Sentinel-2B	27.47123	10:40				
13-Sep-18	Sentinel-3B	32.24380	10:15	58.10301	7:50	23.84465	13:00
	Sentinel-3A	32.13228	10:16				
14-Sep-18	Sentinel-3B	38.04743	9:49	57.93377	7:50	23.72637	13:00
	Sentinel-3A	37.93278	9:50				
15-Sep-18	Sentinel-2A	26.16011	10:40	57.76543	7:50	23.61346	13:00
17-Sep-18	Sentinel-3B	32.20519	10:11	59.87897	7:40	23.40413	13:00
	Sentinel-3A	32.09146	10:12				
18-Sep-18	Sentinel-3B	38.11599	9:45	59.71656	7:40	23.30785	13:00
	Sentinel-3A	37.99984	9:46				
25-Sep-18	Sentinel-3B	32.34856	10:04	58.62343	7:40	22.79475	13:00
	Sentinel-3A	32.23141	10:04				
	Sentinel-2A	23.80906	10:40				
26-Sep-18	Sentinel-3B	38.40783	9:38	58.47502	7:40	22.74462	13:00
	Sentinel-3A	38.28834	9:39				
10-Oct-18	Sentinel-3B	27.41539	10:15	59.15813	7:30	22.61281	13:00
	Sentinel-3A	27.29563	10:16				
	Sentinel-2B	21.34684	10:40				
11-Oct-18	Sentinel-3B	33.68545	9:49	59.05492	7:30	22.63968	13:00
	Sentinel-3A	33.56560	9:50				
14-Oct-18	Sentinel-3B	27.96047	10:11	58.76784	7:30	22.74382	13:00
	Sentinel-3A	27.84065	10:12				
15-Oct-18	Sentinel-3B	34.25261	9:45	58.6799	7:30	22.78576	13:00
	Sentinel-3A	34.13287	9:46				
	Sentinel-2A	20.87697	10:40				

APPENDIX 3 : Aqion Setting Parameters and Result

aqion PRO - 6.4.7

File Run Settings Extras Info

Filename: **Aqiontrial.tmp_pH_1**

pH: 8.27
T [°C]: 26.6

DIC
 Alkalinity
 Open CO2 System

CO2 partial pressure: 3.408 pCO2

Ca	412.1	mg/L
Mg	1290	mg/L
Na	10770	mg/L
K	399	mg/L
Al		mg/L
Mn		mg/L
Amm		mg/L

Chloride: 19354 mg/L
Sulfate: 2712 mg/L
Nitrate: 0.0485 mg/L
Phosphate: 0.033 mg/L

More elements

Fe_total Fe(2) and Fe(3)

Fe(2): mg/L
Fe(3): mg/L

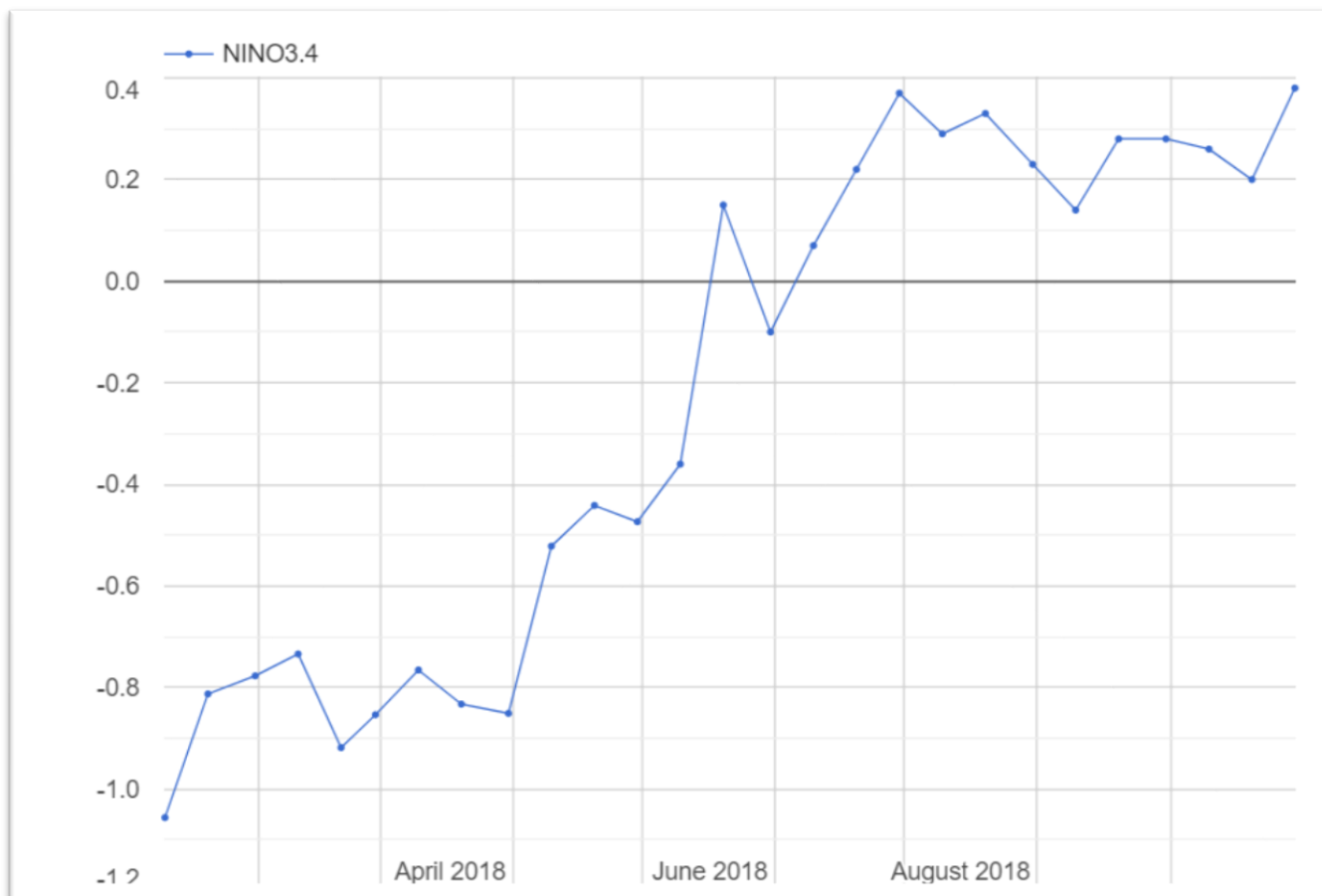
Redox potential

Cr		mg/L
Ni		mg/L
Cu		mg/L
Zn		mg/L
As		mg/L
Sr	7.9	mg/L
B	4.5	mg/L
F	1.3	mg/L
Br	67.3	mg/L
Si	0.365	mg/L
Pb		mg/L
U		mg/L

mol 3 digits		Ions	Minerals	Export	?
		Input	Output 1	Output 2	
	Aqiontrial.tmp_pH_1		pH adjustment	with minerals	
pCO2	-	---	3.41	3.41	
pH	-	8.27	8.21	7.87	
pe	-	4	9.75	10.1	
Eh	mV	238	580	600	
T	°C	26.6	26.6	26.6	
Ionic strength	mmol/L	651	651	650	
TDS	mg/L	35157	35138	35044	
EC at 26°C	uS/cm	53165	53162	53128	
EC_25	uS/cm	51278	51275	51243	
Alkalinity	meq/L	2.63	2.26	0.94	
CH	meq/L	2.63	2.26	0.94	
TH	meq/L	127	127	126	
C.B.E.	%	-0.03	0	0	
DIC	mmol/L	2.28	1.98	0.861	
Ca	mmol/L	10.3	10.3	9.62	
Mg	mmol/L	53.1	53.1	53.1	
Na	mmol/L	468	468	468	
K	mmol/L	10.2	10.2	10.2	
SO4	mmol/L	28.2	28.2	28.2	
Cl	mmol/L	546	546	546	
NO2	mmol/L	0	1.91e-11	1.91e-11	
NO3	mmol/L	0.000782	0.000782	0.000782	
PO4_P	mmol/L	0.000347	0.000347	0.000347	
Si	mmol/L	0.013	0.013	0.013	
B	mmol/L	0.416	0.416	0.416	
Br	mmol/L	0.842	0.842	0.842	
F	mmol/L	0.0684	0.0684	0.0684	
Sr	mmol/L	0.0902	0.0902	0.0902	

		Input	Output 1	Output 2
Calcite	precipitates: 0.66 mM	0	0	0.66
Saturation Indices (SI)				
SI = 0:	Minerals at equilibrium	---	---	---
Calcite	CaCO3	0.82	0.703	0
SI > 0:	supersaturated	---	---	---
Dolomite	CaMg(CO3)2	2.55	2.31	0.935
Magnesite	MgCO3	1.14	1.02	0.35
Talc	Mg3Si4O10(OH)2	3.42	3.05	1.07
SI < 0:	undersaturated	---	---	---
Gypsum	CaSO4·2H2O	-0.669	-0.669	-0.695
Portlandite	Ca(OH)2	-8.79	-8.92	-9.62
Brucite	Mg(OH)2	-2.09	-2.22	-2.89
Hydroxyapatite	Ca5(PO4)3OH	-0.057	-0.251	-1.53
Sr(OH)2	Sr(OH)2	-15.6	-15.7	-16.4
SrF2	SrF2	-5.51	-5.51	-5.51
Strontianite	SrCO3	-0.46	-0.577	-1.25
Celestite	SrSO4	-0.661	-0.661	-0.658
Fluorite	CaF2	-1.4	-1.4	-1.43
Halite	NaCl	-2.54	-2.54	-2.54
Thenardite	Na2SO4	-3.21	-3.21	-3.21
Mirabilite	Na2SO4·10H2O	-2.57	-2.57	-2.57

APPENDIX 4: El-Nino Index in Indonesia on 2018.



Source: (Indonesia), 2019)